PERDIKA 2

Archaeological Background

Perdika 2 is a recently discovered site identified during an archaeological survey of the area. It is located on a steep hill northwest of the nearby prehistoric settlement of Perdika 1. Surface material indicates that Perdika 2 was active during the Middle Neolithic period. In general, the material is more dispersed compared to other prehistoric settlements in the study region. The position of the site on a steep hill, and not directly within the lower plains, may indicate a difference in the mode of human activity that developed here.

Satellite Remote Sensing and Historical Aerial Photography Survey

A GeoEye-1 image from 3 June 2010 was used for satellite remote sensing at Perdika 2 (Figure 1). The satellite image has an off-nadir angle of 9.8° and a ground sampling distance (GSD) of 0.50 m (panchromatic) and 1.92 m (multispectral). In addition to the satellite imagery, two historical aerial photographs were used for remote sensing. One was taken in 1971 (date unknown) with a scale of 1:10,000, and another on 22 August 2003 with a scale of 1:30,000 (Figure 2).

The broader landscape around the prehistoric site is diverse and characterized by flat agricultural floodplains, large river and stream beds producing deep gorges, and mountains on the western and northern peripheries. A few modern villages and roads pocket the terrain, but for the most part the region is devoid of modern constructions and farming facilities. At just over 1 km in distance, Perdika 2 is close to the nearby prehistoric settlement of Perdika 1 to the south. However, the local topography of the two settlements varies greatly. Perdika 2 stands on a natural hill that towers over the surrounding landscape, providing an excellent vantage point of the wider floodplain below. The western side of the settlement has a precipitous ravine, while the eastern and southern sides have steep slopes. During the extraction date of the 3 June 2010 GeoEye-1 imagery, most of the agricultural fields were recently harvested, apparently for wheat. As a result, there is limited green vegetation in the satellite imagery within and around the site. Elevations around the target range from 300-320 masl. This is around 50 m higher than the settlement of Perdika 1.

A comparison of the aerial photo from 1971 with the 3 June 2010 GeoEye-1 indicates that the landscape around Perdika 2 has changed slightly in the 40 year period between the two images. Portions of the forested mountains north of the site have been carved out and converted into agricultural fields for the cultivation of wheat. The field boundaries of some agricultural fields have also changed. The quality of the 22 August 2003 aerial photo is too grainy to evaluate in the same context.

Satellite remote sensing around Perdika 2 produced modest results (Figures 3-4). The majority of features correspond to palaeochannels (blue) associated with the rivers and streams that pocket the terrain. This is not surprising given the steep landscape around the prehistoric settlement. Other anomalies seem to relate to agricultural activity (brown), such as former field divisions and plow lines. A third category of anomalies is unclassified (yellow). The majority of these

anomalies have globular and roughly circular formations and likely relate to small lakes from seasonal flooding or designate the courses of former river beds.

Two faint circular or near circular anomalies were detected in harvested wheat fields at Perdika 2 separated by about 250 m (Figure 5). Anomaly #39 is not quite a full circle and is located on the adjacent hilltop east of Perdika 2. PCA, TSAVI, and MSR best depict this anomaly. Surface pottery is abundant on this hill. Anomaly #45 is marginally better represented and is roughly 120 m in diameter. Decorrelation Stretch is the optimal spectral filter for identifying its parameters. Although Anomaly #45 stands on the prehistoric tell, it is further south from where geophysical prospection (see below) has mapped the main area of the settlement. No other surface anomalies around Perdika 2 seem particularly good candidates for features of archaeological interest.

Figure 1: GeoEye-1 coverage of Perdika 2

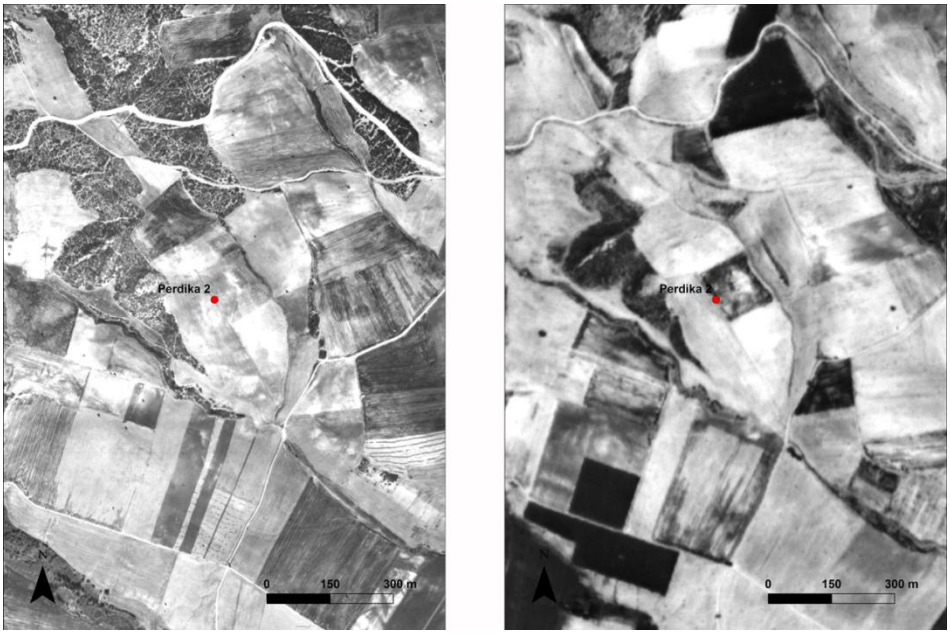

Figure 2: A comparison of historic imagery

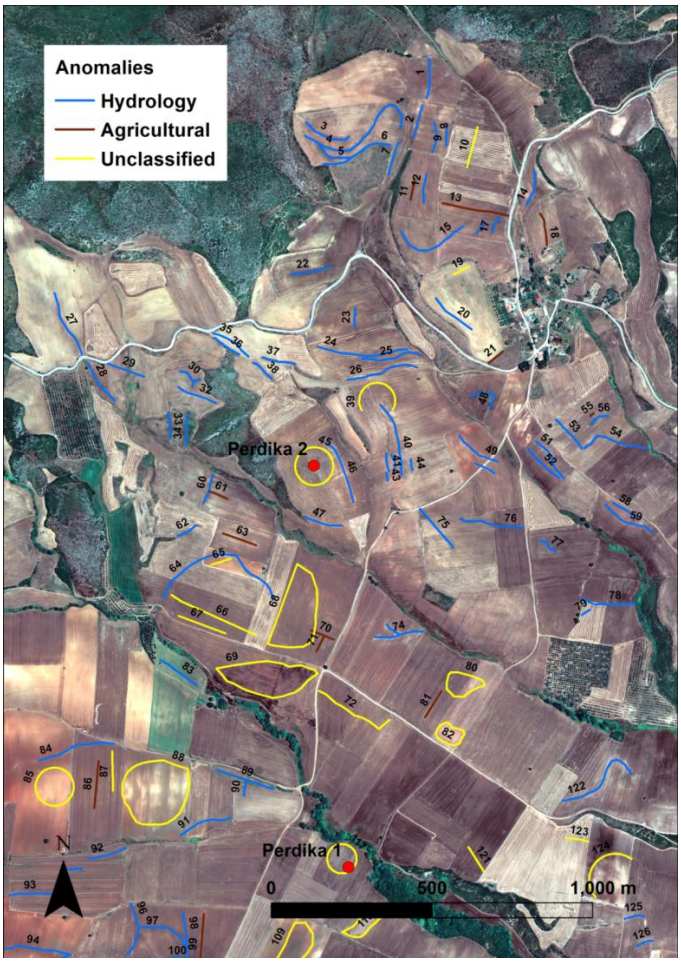

Figure 3: Anomalies detected on satellite imagery

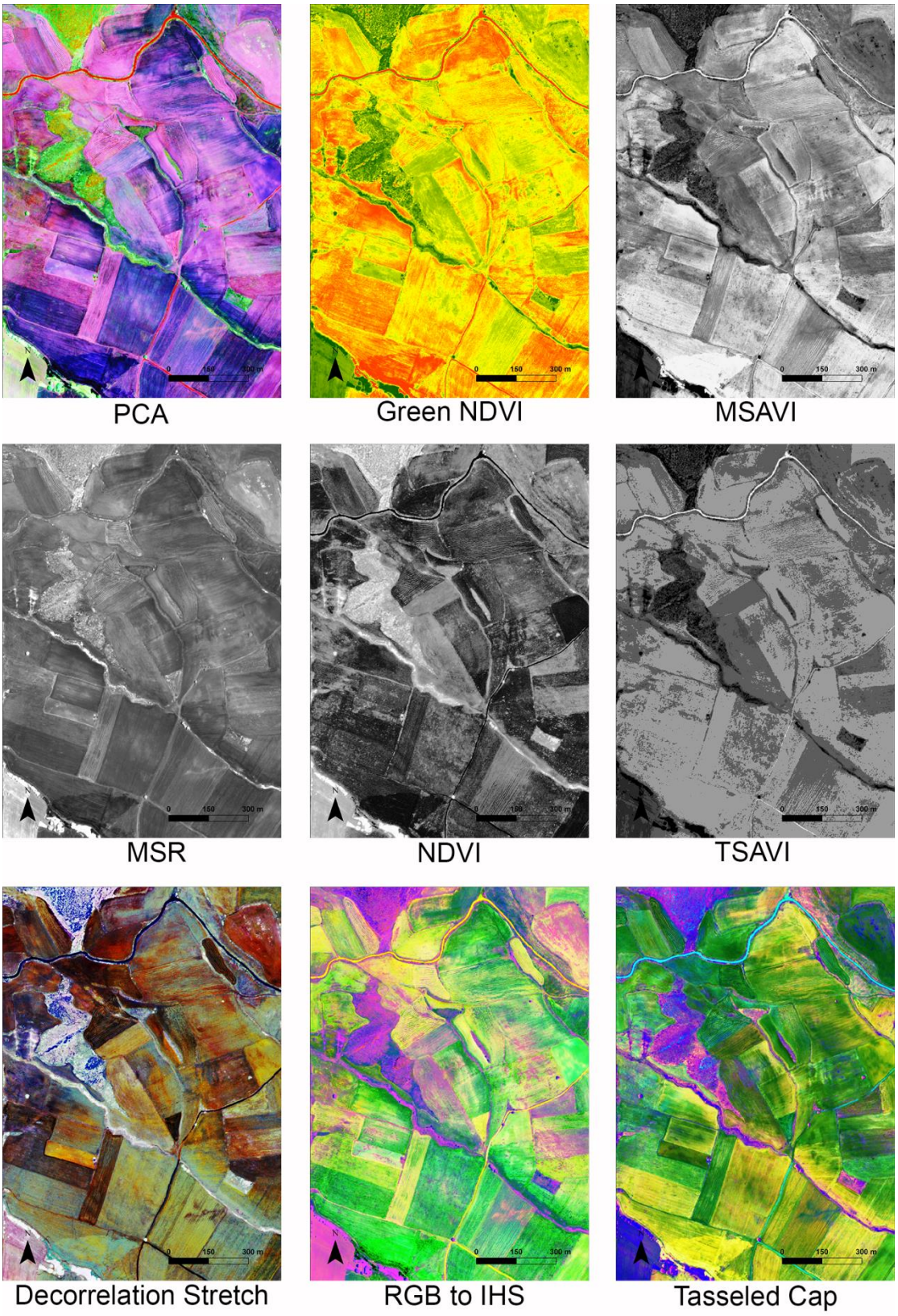

Figure 4: Satellite remote sensing products for the detection of anomalies

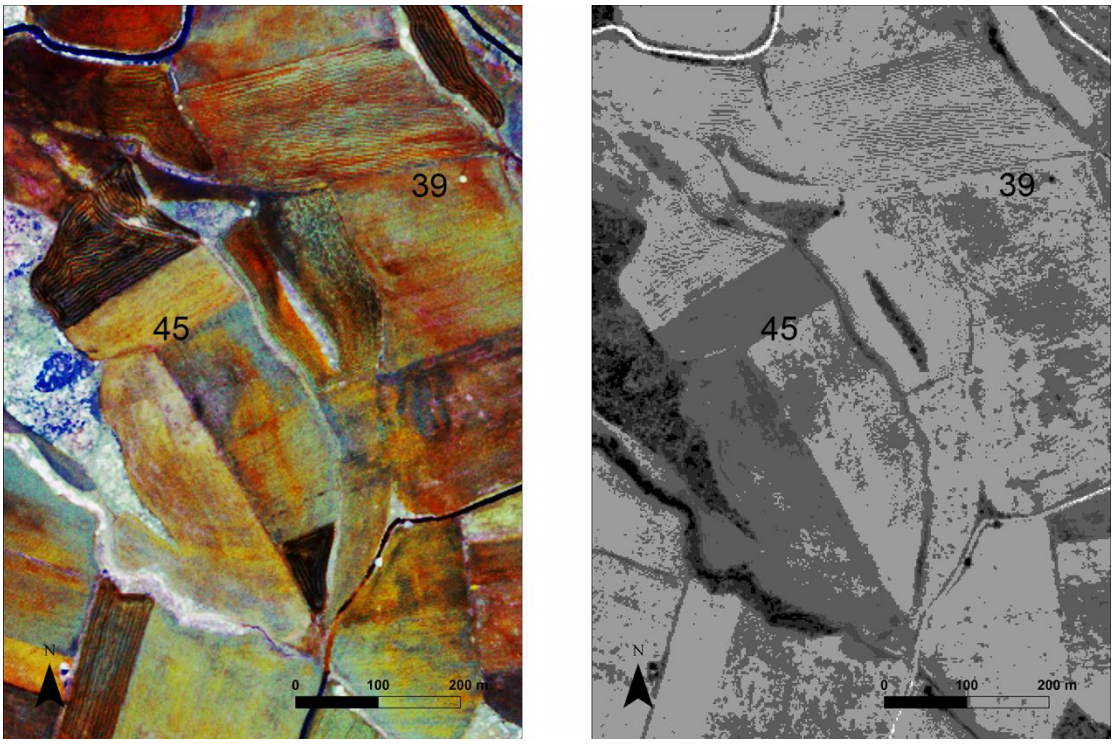

Figure 5: A focus on two anomalies related to the site

Remotely Piloted Aircraft Systems (RPAS) Survey

The low altitude photogrammetric documentation of Perdika 2 was undertaken over the course of several flights and at the same period as fieldwork for Perdika 1 (15-20 October 2014). The field conditions here were also the same as Perdika 1. For these reasons, no real features could be identified in the computer aided visualization of single photo-frames or composed orthophoto of the area, due to the recent ploughing.

More interesting results were extracted from the satellite imagery, available online through web map service (WMS) services. In particular the orthophoto from the National cadaster service ("Ktimatologio") provides a good amount of linear features, impressively matching with the geophysical interpretation of collected field data; also helping the RPAS data analysis.

A close-up comparison between linear anomalies from geophysics (Figure 6b) and the dark lines on the orthophoto seem to perfectly match. What remains unclear, however, is the nature of these lines from photo interpretation. The fact that they are darker than the surrounding vegetation may suggest higher water retention, meaning that they probably are the result of ditches filled with different or less compact soil. At the same time, analogous visual output may also be produced by geological layers of different consistency or materials (see for example the image below (Figure 7), although from a different geographical context).

These geologically derived features are also visible in close-by fields more to the south of the settlement, although the chromatic differentiation is not so sharp as for the dark lines matching with the geophysical analysis.

A further interesting area is the field on the southeastern side of Perdika 2, about 300 m from the center of the settlement's summit. A number of features seem to be recognizable in that area,

some probably belonging to geological layers, some to potential anthropic activity. The particular shape of the latter one (the dark line in Figure 8) with its sharp narrow edges and sudden turn (where the median red arrow is in Figure 8) seem to allow its possible association with anthropic activity, rather than being the result of geological outcrops.

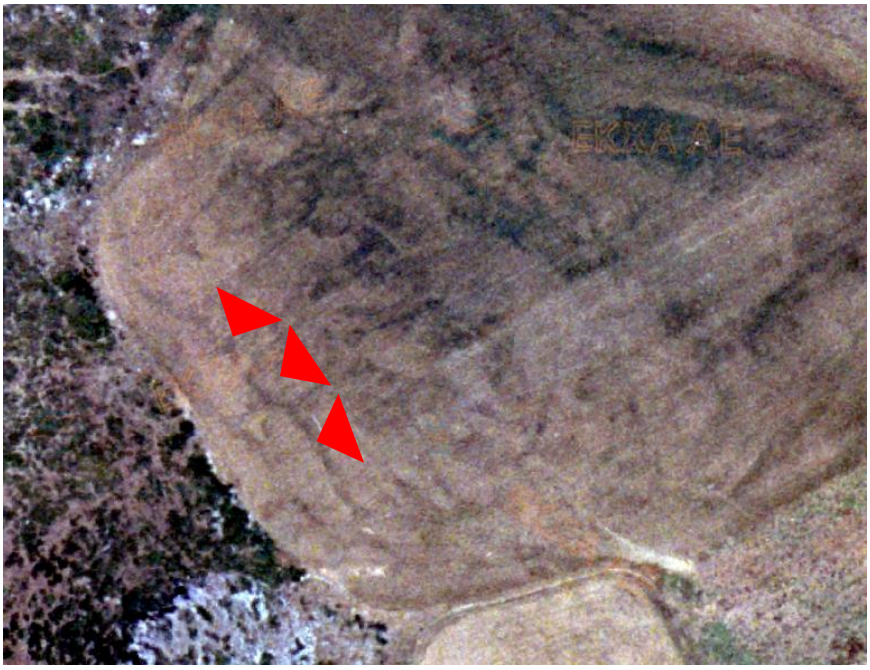
(a)

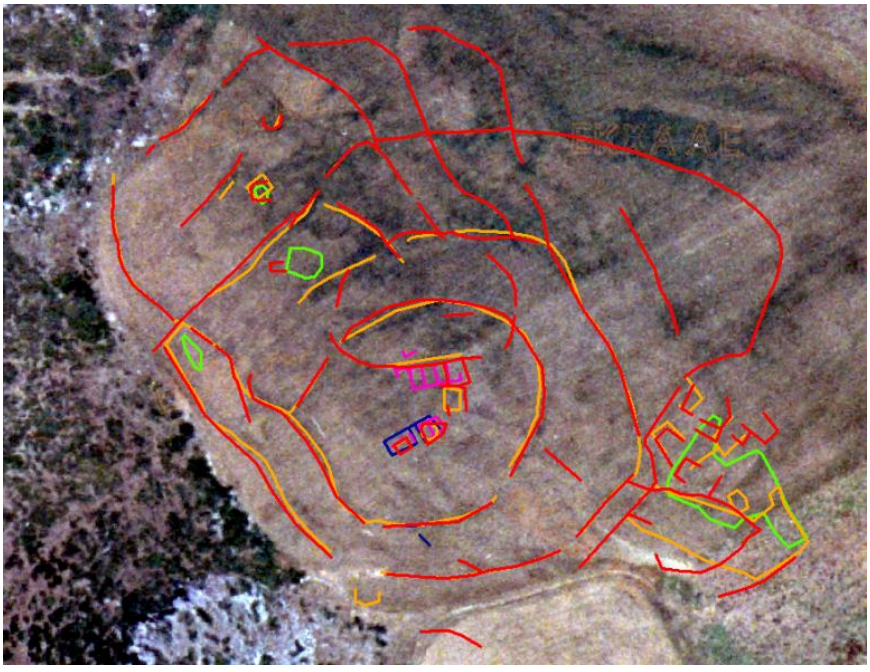
(b)

Figure 6: Above (a) the orthophoto from the Ktimatologio showing up a number of linear features (one of which is highlighted with arrows) in correspondence with the geophysical mapping (b).

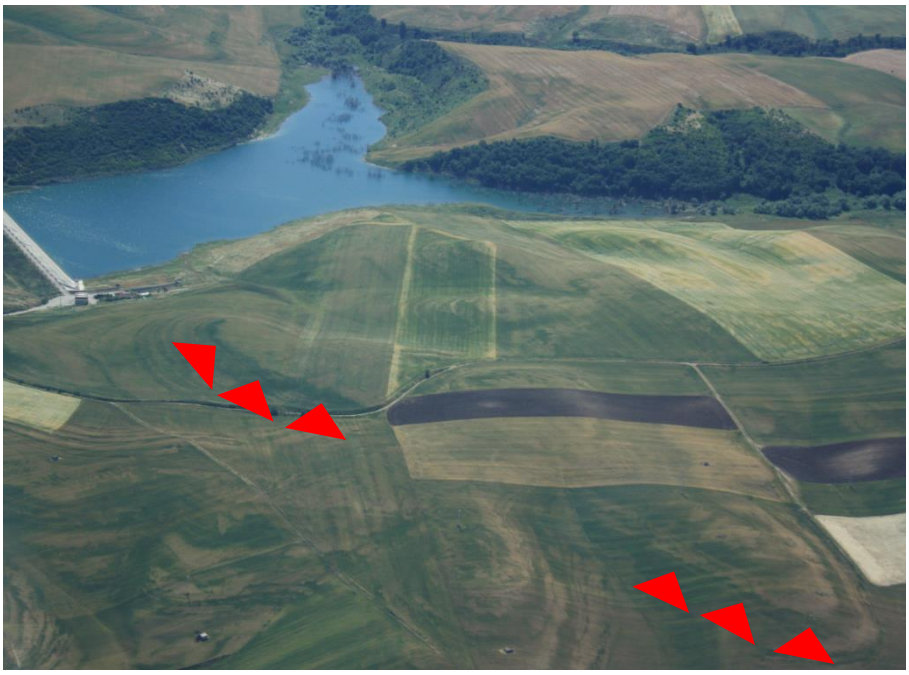

Figure 7: Linear features (some of which highlighted with red arrows) due to layered geology. Example of darker lines (due to different water retention of layers) from Southern Italy.

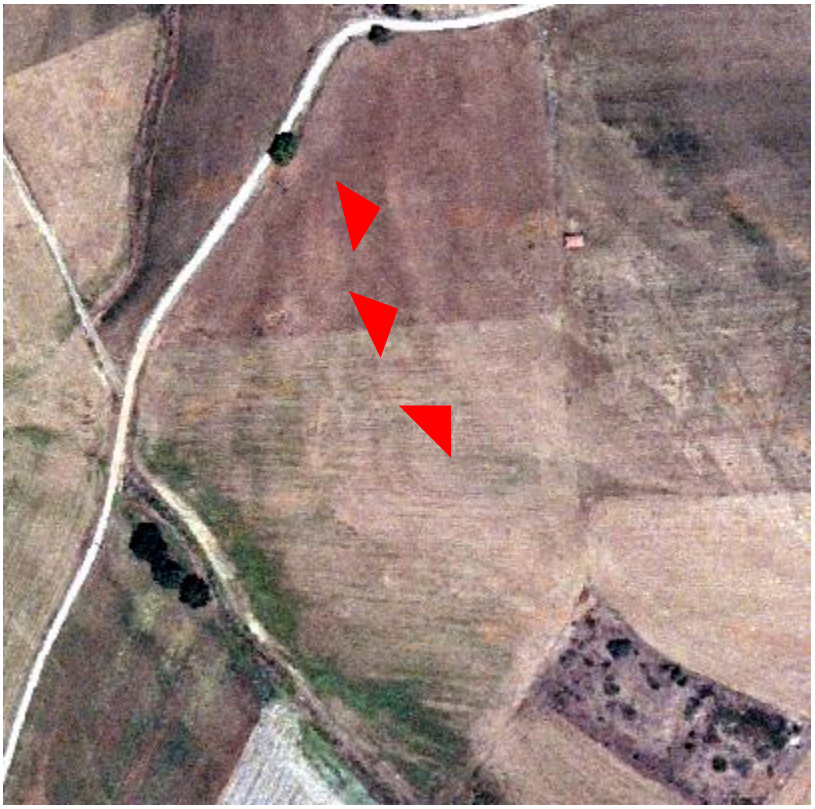

Figure 8: Geologically derived linear features in field-plots about 500meters South-East of the magoula.

Figure 9: Example of possible coexistence of geological (lighter linear features, green arrows) and man-made features (sharpe linear darker line making a kind of an angle, see red arrows).

This last area (Figure 9), with the coexistence of features with natural origins and potentially man-made objects, helps clarify the structure and use of the settlement. It is possible that man-made structures were somehow connected with the local topography and geology in a way that walls could have been built right above rocky or stony outcrops. They may have been surrounded by ditches, most probably on one single side.

Geophysical Prospection

Geomagnetic Survey

Geomagnetic data reveals a complex "plan" of the site. Multiple settlement cores and enclosures indicate various occupation and even cultural phases. However, the data does not provide clear traces of architectural details. Though it is hard to provide definite chronologies due the nature of geophysical prospection, some of the occupational history of the settlement can be suggested based on superimposition of magnetic anomalies.

The magnetics survey reveals three different settlement cores. The core (C1) that also contains A21 is the smallest and surrounded by the enclosure A3 (see the EM data for a better representation of this phenomenon). The second settlement core (C2), located immediately to the north of A21, is larger and appears to be cut by A3. We believe this settlement core to be earlier than the first core. The third core (C3), the largest of all, is located to the east and bears no

spatial relationship with the first two; therefore, it should be evaluated independently. Here, there are no immediately visible architectural elements, but the heterogeneity of data suggests that the area is of anthropogenic origins.

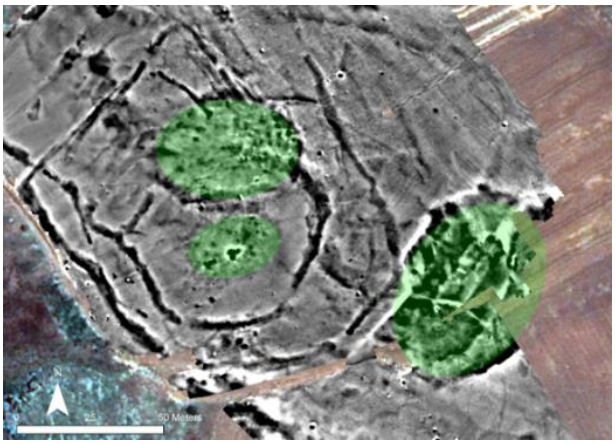

Figure 10: Detected settlement cores

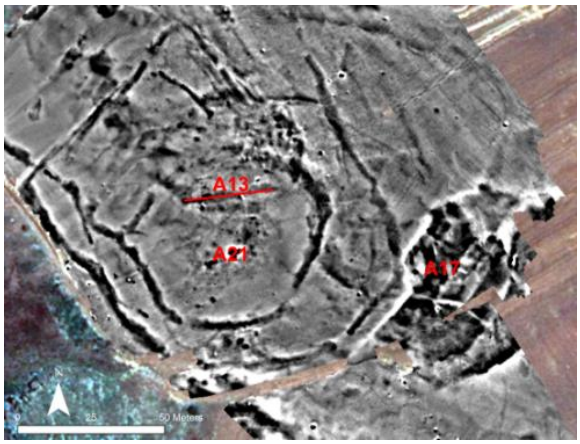

Figure 11: Related annotations

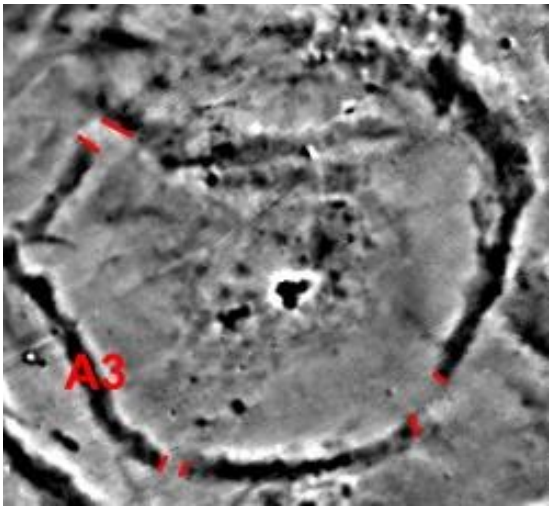

Figure 12: Enclosure openings detected in the geomagnetic data

Alternatively, there are two settlement cores (represented around A17 and A21), and in fact A13 divides C1 into two main clusters. If A13 is indeed a partition, then it is highly possible that it was also used as a retaining wall for the contiguous structure (A22), which is only visible in the GPR data. Considering the ambiguity of interpreting settlement cores, we also have to investigate enclosures.

A3 surrounds A21 and A22, and it makes a sharp angle in the northwest corner. The enclosure has three openings located in an orthogonal fashion. It is not clear whether there existed another opening at the northern side of enclosure A3. It is also likely that the western opening of A3 has a feature at the upper side that abuts A13, and, therefore, is architecturally connected to A22.

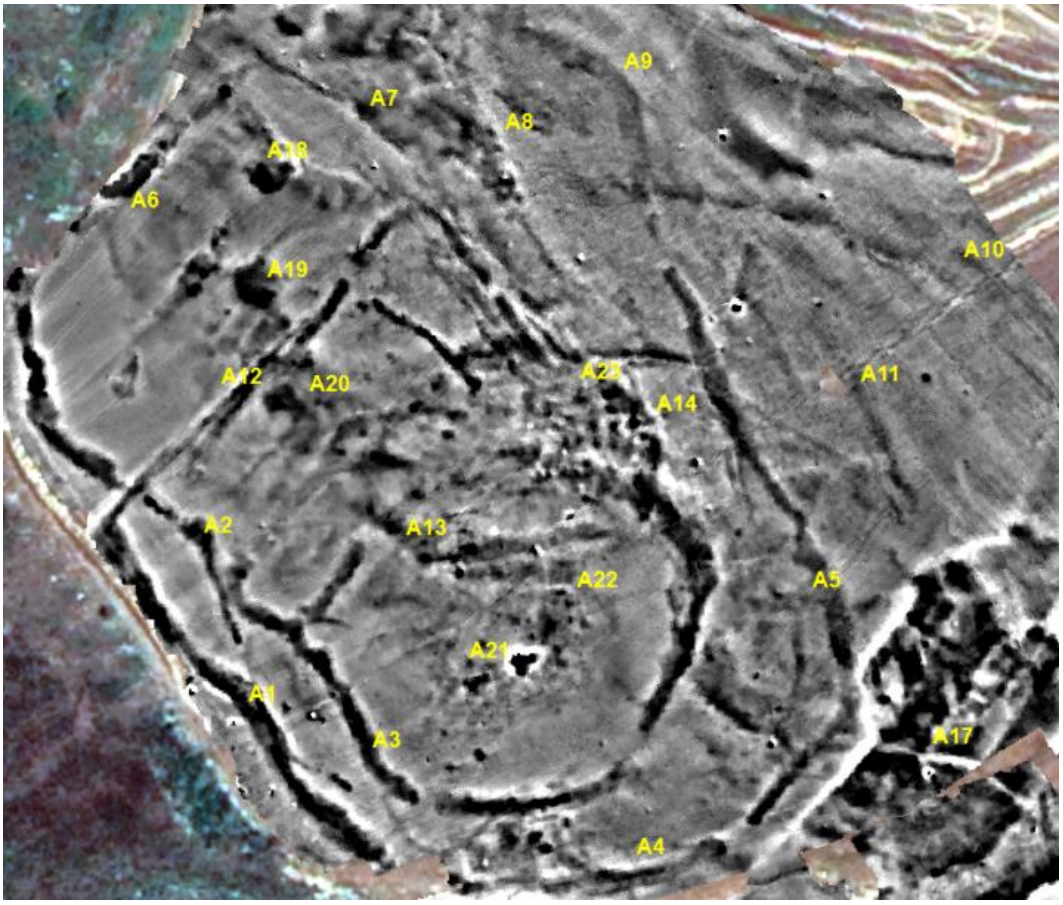

Figure 13: A complex set of anomalies detected on geomagnetic data

A2 and A6 together with A3 form another enclosure around C1 (and potentially C2). A8 and A9 appear as extensions and are parallel to A7. However, A9 presents a curious case as it could be a part of the series of anomalies A5 and A4. If A4 does not terminate at the southern edge of A3, instead continuing as A1 (and later on A12,) then what we see is a spiraling enclosure which is not completely uncommon in Neolithic. Nonetheless, this point of the interpretation remains speculative. We can also suggest A1, A12, and A10 as another enclosure, although with a completely different spatial arrangement. If correct, then this arrangement suggests an orthogonal rotation of enclosures, and it is unlikely that it would happen in the same architectural phase. This possibility also raises the likelihood of a second settlement core within the complex set of enclosures (see the discussion above for C1 and C2).

Electromagnetic Induction Survey

EM measurements were done on the site of Perdika 2 with the GEM-2 from Geophex. It was used with a GPS unit, acquiring simultaneously the location of the point and the value of the EM field for five different frequencies (from 5 kHz up to 90 kHz). Only the first two frequencies were used to extract from the raw signal the value of the complex magnetic susceptibility and the electrical conductivity. As the coil spacing is 1.6 m and the coil geometries used is HCP we have 2.5 m depth of investigation for the electrical conductivity and 1.6 m for the complex magnetic susceptibility. The instrument was carried at an elevation of 0.3 m. We covered an area of 1.96 ha, done in one and half days by two surveyors.

The complex magnetic susceptibility is presented through the map of the magnetic susceptibility (or the real part of the complex magnetic susceptibility) and the magnetic viscosity (or the imaginary part of the complex magnetic susceptibility). Depths of investigation are the same for both magnetic properties.

We also used the CMD Mini-Explorer from GF Instrument. Data acquisition was based on several grids to localize the points. We did a profile every 1 m, allowing a characterization adapted for archaeological targets. We obtained twelve maps corresponding to three depth of electrical conductivity and three depth of magnetic susceptibility. The CMD was used in a HCP and VCP configuration. It allows a multi-depth characterization. Table 1 shows the different depth of investigation of each map. Each depth corresponds to a slice of soil from the topsoil up the indicated depth. The instrument was carried at an elevation of 0.3 meter. This data acquisition was done as a test to assess the benefit of a muli-depth characterization. The grid covers an area of 0.24 ha.

Coils spacing	Coil geometries	Electrical Cond.	Magnetic Susc.
0.32	HCP	0.5	0.3
0.72	HCP	1	0.7
1.3	HCP	1.9	1.3
0.32	VCP	0.3	0.4
0.72	VCP	0.7	0.9
1.3	VCP	1.3	1.5

Table 1: EM Parameters List

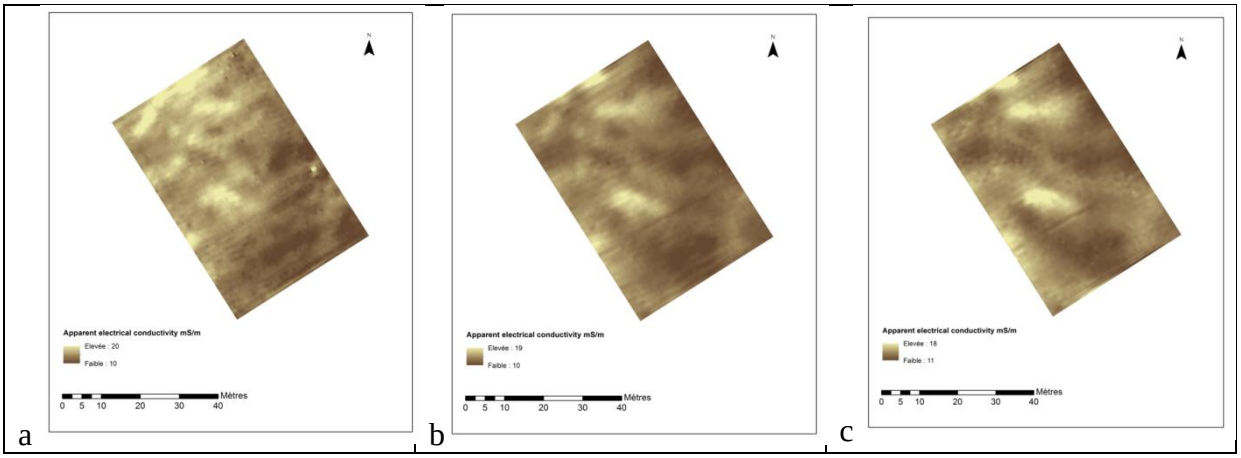

a b c

Figure 14: Apparent electrical conductivity (CMD Mini Explorer – HCP): coils spacing a-0.32; b-0.72; c-1.3

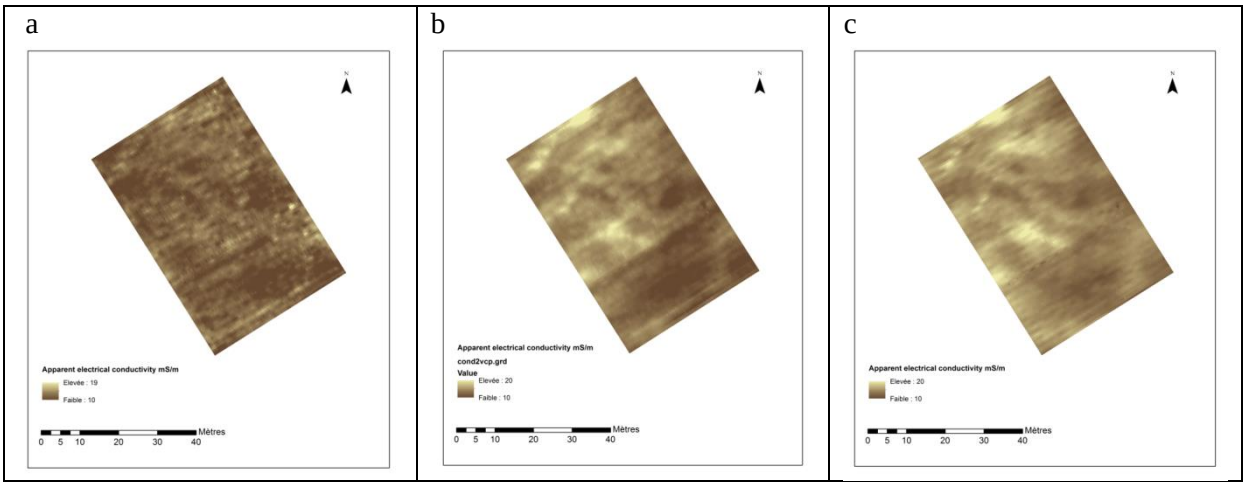

Figure 15: Apparent electrical conductivity (CMD Mini Explorer – VCP) coils spacing a-0.32; b-0.72; c-1.3

The electrical conductivity data does not reveal any clear anomalies. We observe some higher valuse of conductivity (close to 20 ohm.m), but these anomalies do not identify any clear archaeological targets. Regarding the geometrie used to do the meausrement, HCP data are less noisy than VCP. In the case of VCP measurements, the data shows a strong profile effect for the three different depths. This effect was easily processed for the HCP configuration. As this map did not show any valuable information for archaeological prospection, it is not easy to speak about the multi-depth characterization.

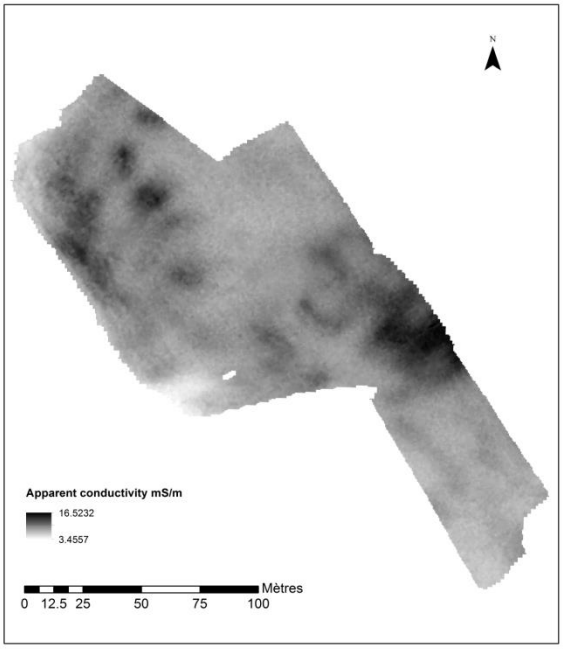

Figure 16: Apparent electrical conductivity (GEM2 – HCP)

The electrical conductivity measured with the GEM-2 reveals a low conductivity. Regarding the previous data recorded with the CMD, we can see a decreasing of the apparent electrical conductivity with the depth. This decreased values probably are a result of the bedrock under the

topsoil. In this configuration, the map of electrical conductivity shows several traps accumulating soil material. It would be useful in the future to do some coring and try to date the archaeological layers in this steep area. The conductive anomalies are almost all leaning againt magnetic linear anomalies interpreted as walls. Towards the east, the bigger conductive anomalies could relate to a geologic disturbance also visible on the magnetic map (for both EM and magnetic measurement).

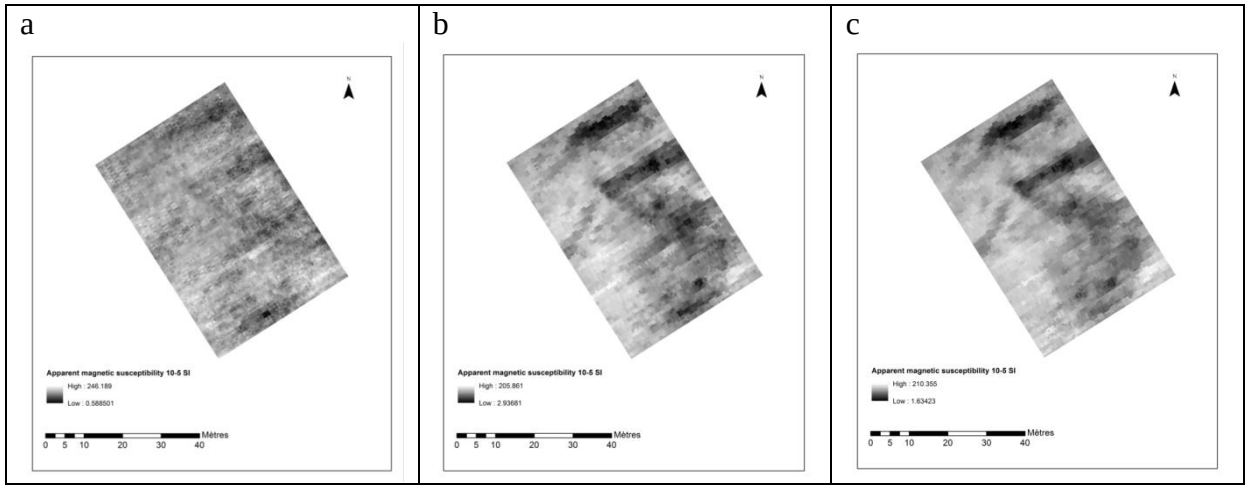

Figure 17: Apparent magnetic susceptibility (CMD Miniexplorer – VCP) coils spacing a-0.32; b-0.72; c-1.3

The magnetic suscpetibility from the CMD reveals more information than the electrical conductivity. In this case VCP measurents were clearer than HCP measurement. The test was done on the core of the site, centered on the building found with the other method (GPR and magnetic survey). Even if walls are not visbile, we can clearly observe the magnetic linear anomalies. For the first depth of investigation, the double linear anomalies are visible, even if these features are not clear and the map presents a homogeneous disturbance corresponding to the heterogeneities of the plough soil. Beginning at 1 m in depth up to 1.5 m, we can follow both linear anomalies and also larger anomalies in the south. Inside this larger anomaly, we can also observe a few local and strong magnetic anomalies.

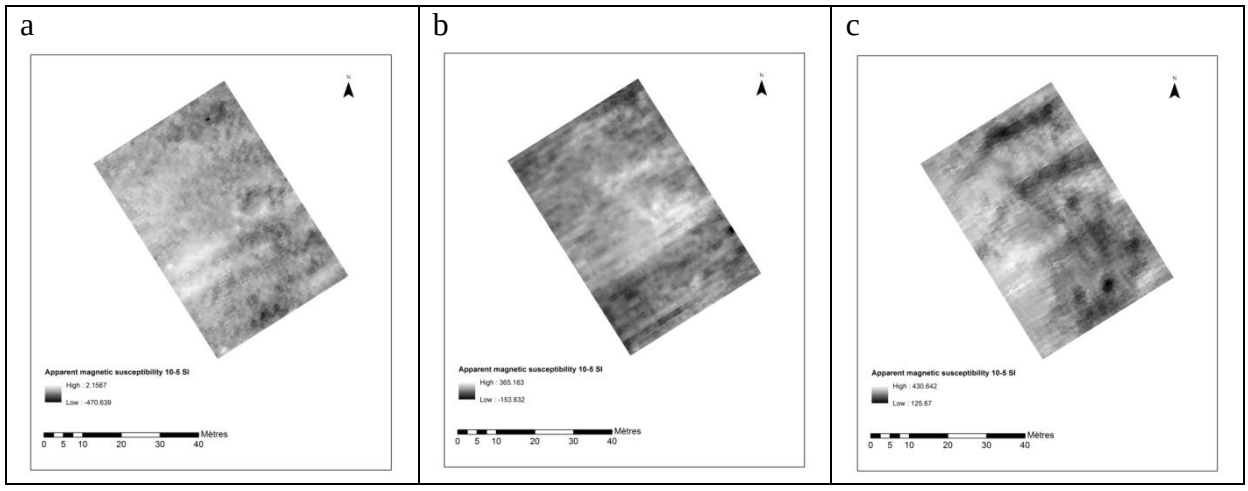

Figure 18: Apparent magnetic susceptibility (CMD Miniexplorer – HCP)

The measurement of the magnetic susceptibility done with the CMD in an HCP mode are less clear than in VCP configuration; nevertheles, it does show an interesting misunderstanding of the HCP measurement. The deeper layer shows a map very similar to the VCP measurement. We can follow the two linear and interrupted anomalies as showing by the magnetic data. The dataset reveals also some local anomalies corresponding to burning place or similar archeological artefact. But for the intermediate depth, the two magnetic linear anomalies seem to be amagnetic. This effect comes from the inversion of the magnetic anomalies measured with an HCP configuration. The use of several depth of investigation allow to control this effect here, but we can easily understand the possible misunderstanding in another case without a multi-depth caracterization.

The first depth of investigation is only affected by the very near surface topsoil and any archaeological feature can be observe here. In this case we can say than the magnetic anomalies are appearing at a depth of 0.4 m and are expanded until 1.6 m. The only magnetic susceptibility is not enough to say if it's a wall or a ditch.

The map of magnetic susceptibility resulting from the measurement with the GEM-2 in HCP mode is very clear and close to the results of the magnetic survey. We observe several linear magnetic anomalies ditributed around the core of the site. On the central part, we see a diffuse anomaly of magnetic susceptibility matching the GPR result. This central area is probably an area related to the building and domestic life of the settlement. The linear anomalies present different interruptions corresponding probably to an entrance system.

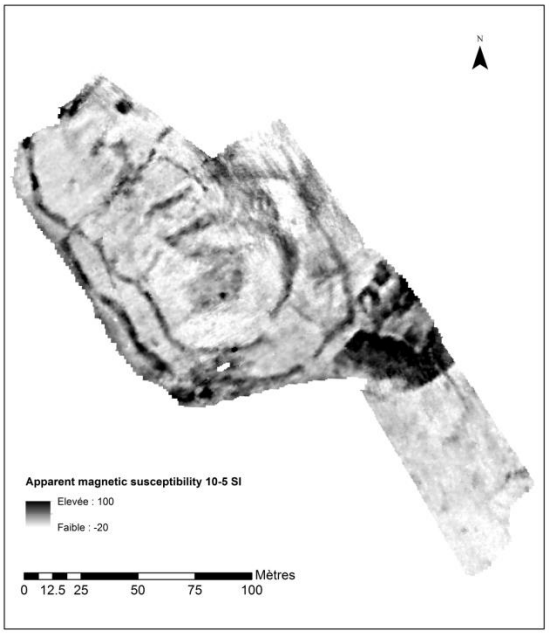

Figure 19: Apparent magnetic susceptibility (GEM2 – HCP)

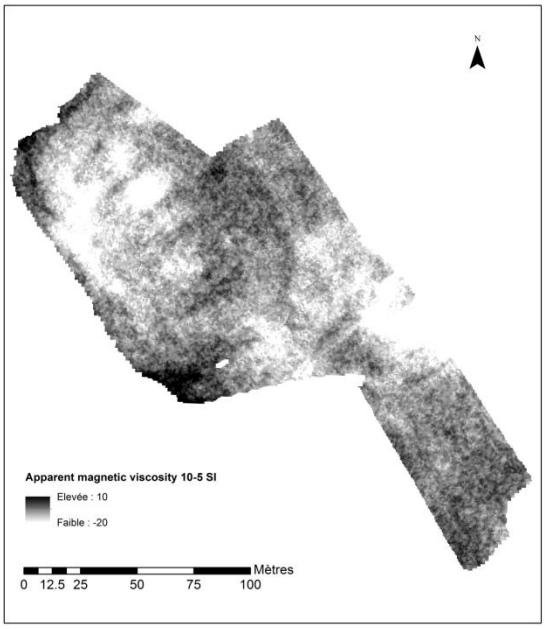

Figure 20: Apparent magnetic viscosity (GEM2 – HCP)

The map of the magnetic viscosity shows very interesting information. In this specific case, we can follow different anomalies corresponding with the electrical conductivity (in white) and with the magnetic susceptibility (the black linear anomalies). But we can see on the center of the site a global higher value of magnetic viscosity corresponding to the central enclosure and concentrated in the north part of this area. At this point, it is very difficult to give a clear interpretation of this higher value, but it likely corresponds to a specific soil treatment like gardening, animal husbandry, etc. This point needs to be confirmed by soil analysis.

Ground Penetrating Radar Survey

The results obtained by Noggin Plus Smart Cart are summarized in Table 2. The total area covered was 3200 m^2 and consisted of three survey grids. The grids were set on a relatively flat area at the top of the natural hill. The data were processed as follows: Trace reposition, Repick first break (5%), Dewow, SEC2(Atn=34.05 dB_m,StrtG=3.35,MaxG=226), Background average subtraction, Bandpass filter (Fc1=120 % Freq,Fp1=160 % Freq,Fp2=200 % Freq,Fc2=240 % Freq), Background subtraction (FW=1.0 m, Type=rectangular). In this case, GPR did not manage to locate the enclosures that are visible both in the magnetic and EM results, but it did map a prolonged structure that appears as a strong anomaly and is not visible in the results of the rest geophysical methods. The structure is presented in the 3D GPR cube in Figure 5. Besides this feature, no other anomalies are clear in the results, indicating either a blank area or a low contrast in the material's electrical properties.

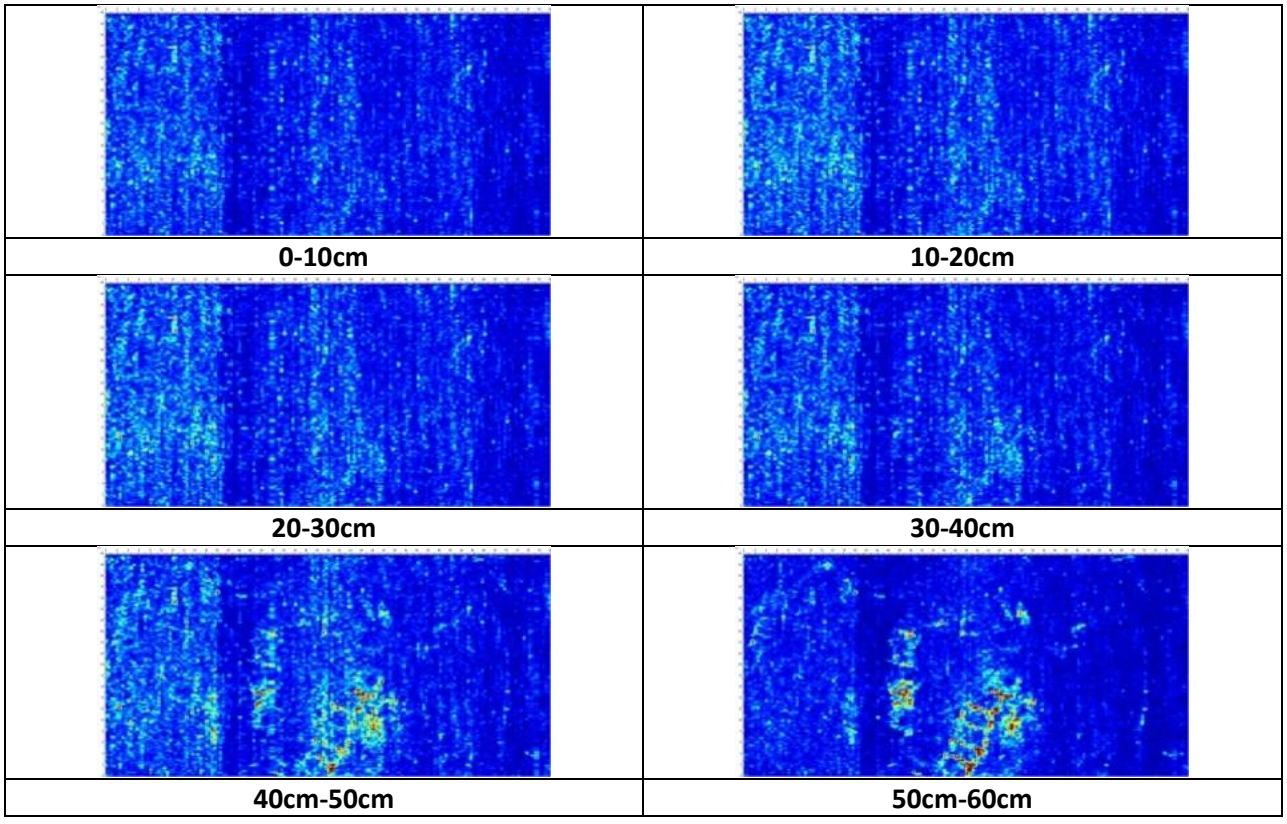

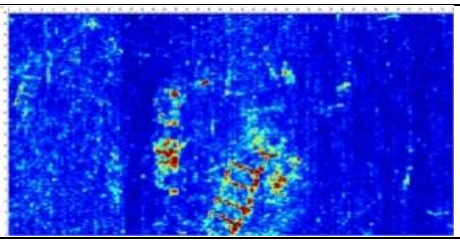	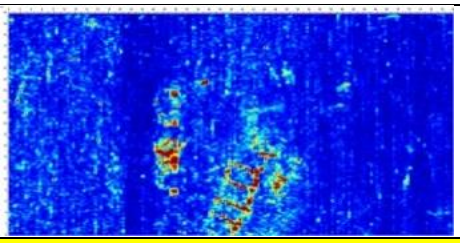
60cm-70cm	70cm-80cm
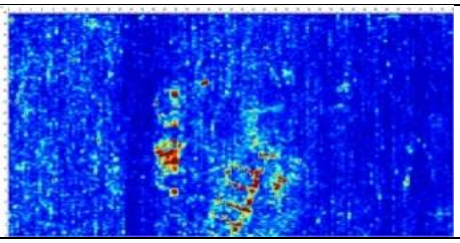	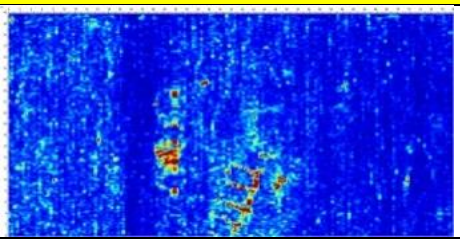
80cm-90cm	90cm-100cm
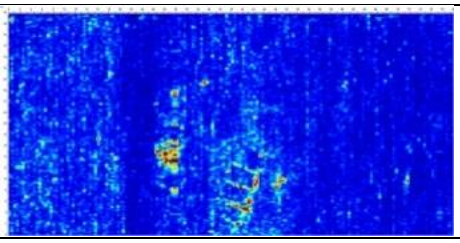	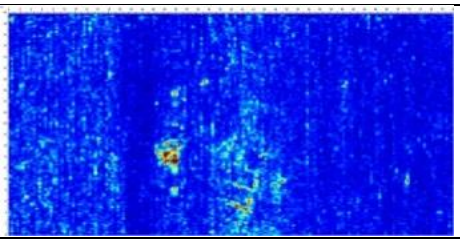
100cm-110cm	110cm-120cm
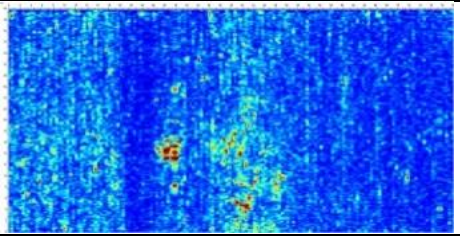	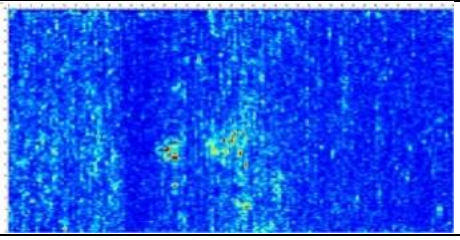
120cm-130cm	130cm-140cm
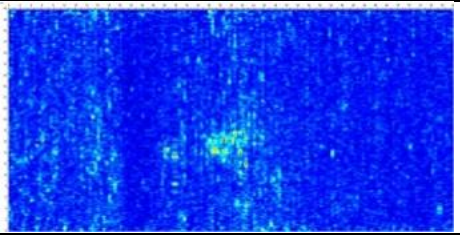	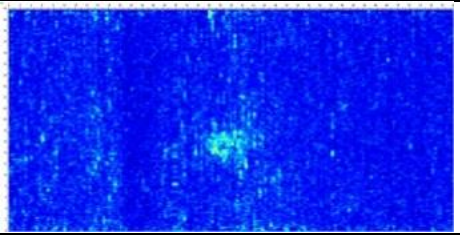
140cm-150cm	150cm-160cm
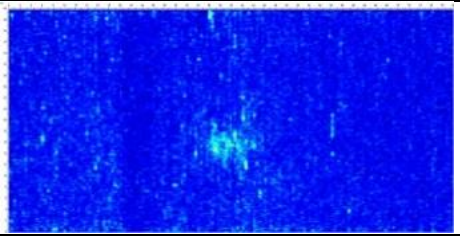	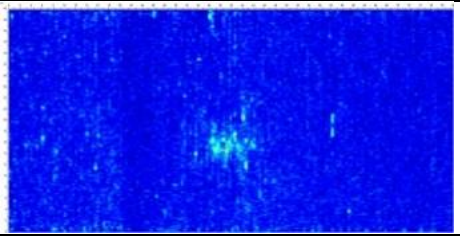
160cm-170cm	170cm-180cm

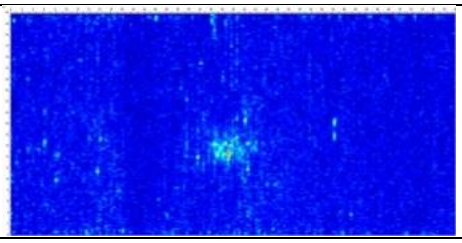	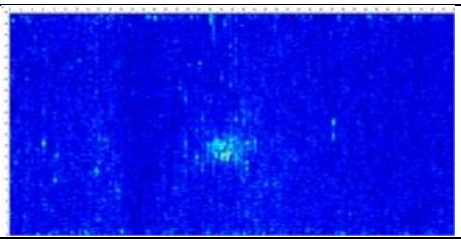
180cm-190cm	**190cm-200cm**

Table 2: GPR depth slices for the grids with code name PER1 to PER2, at Perdika 2 with 10cm thickness.

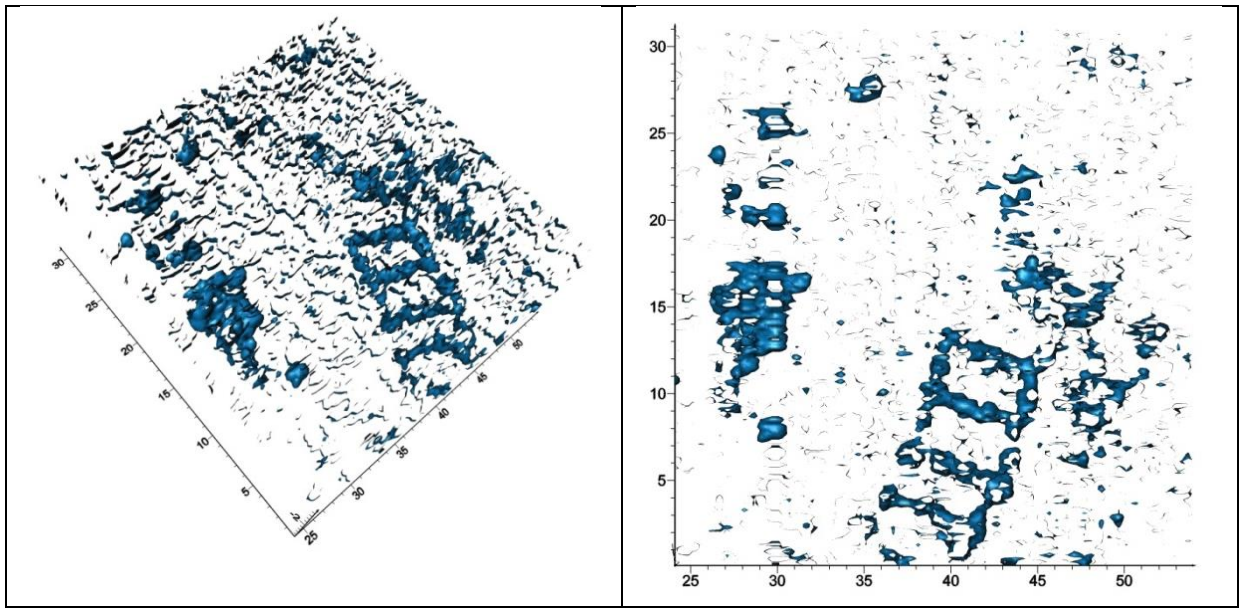

Figure 21: Different perspectives of the GPR 3D cube were the strongest reflections are isolated.

A representative GPR slice is presented In Figure 22 along with the magnetic results and the corresponding interpretation. The reflection A22 indicates a prolonged structure that appears at a depth of 50-100 cm. The dimensions of the structure are approximately 13 m by 5 m, and there are at least three-five rooms measuring 3.5 m x 5 m. Another two anomalies were also identified close to A22, although it is not clear whether they are related with A22 or if they are fragments of demolished individual structures. The fact that these features are not visible in the magnetic and EM results indicates different construction material than the enclosures. The group of reflections A21 is also visible in the resistivity and magnetic results as strong anomalies. In GPR slices they appear within the same range as A22, indicating the structural remains either of two demolished structures or parts of a prolonged structure similar to A22.

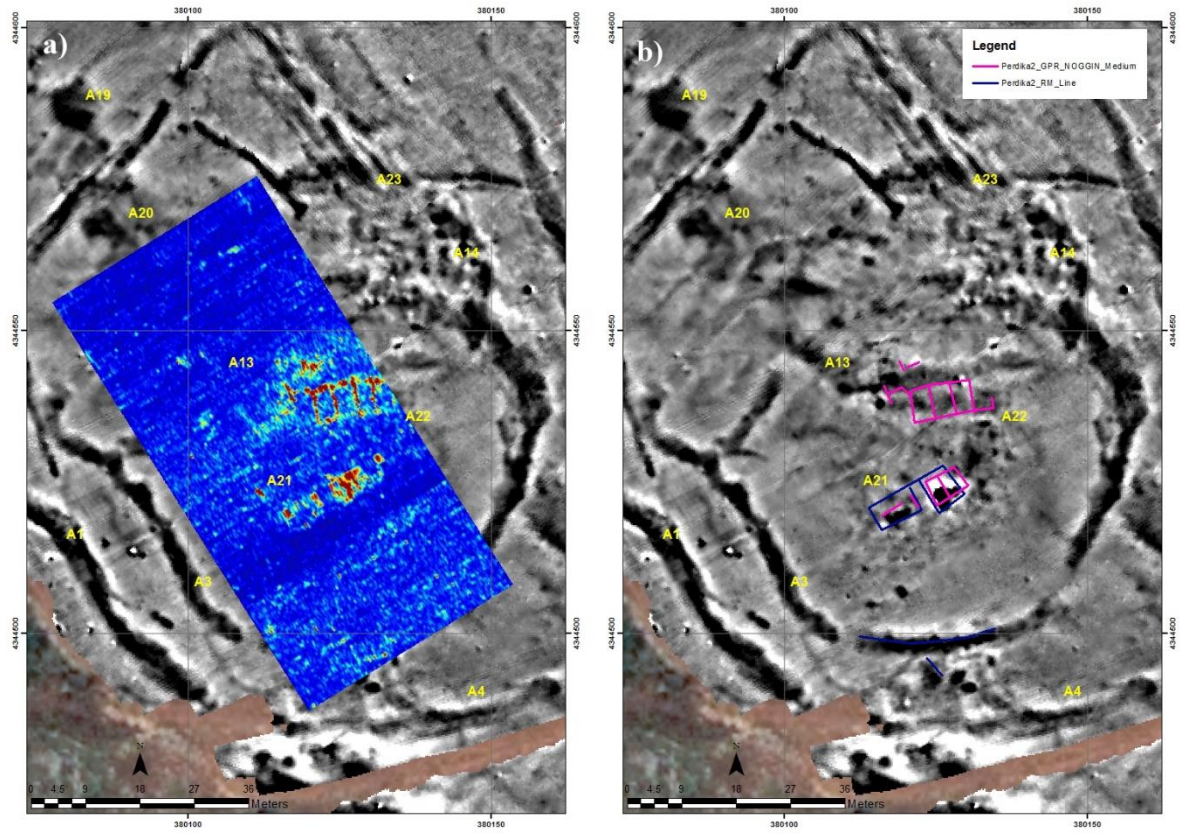

Figure 22: Georeferenced GPR slice superimposed on the magnetic results, where a) is the slice at 70-80 cm depth while in b) the strongest GPR anomalies are outlined and presented along with the high resistivity anomalies.

Resistance Survey

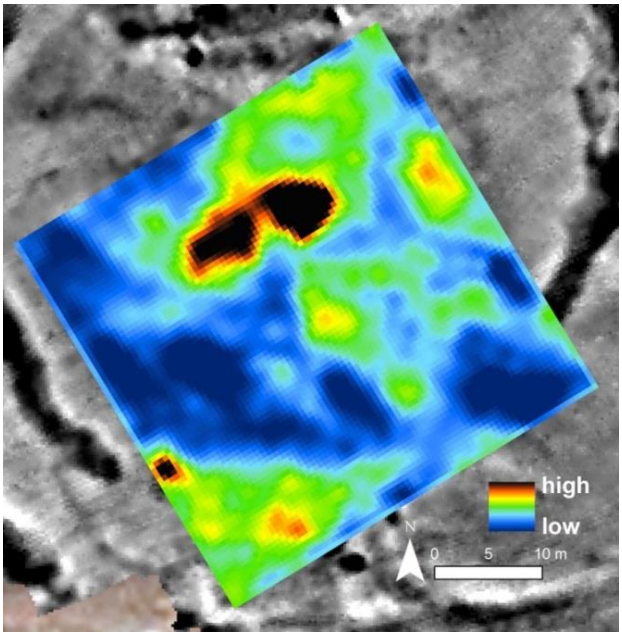

Figure 23: Results of the resistance survey

The resistance survey in Perdika 2 was informative with respect to the magnetic data. In the south of the survey grid, we observe a sharp division between resistivity values which also correspond to anomaly A3, supporting the idea of a built enclosure rather than a ditch. Furthermore, the high resistance feature at the northwest corner aligns well with the opening of this built enclosure, suggesting a "gate-like" feature for the inner-core of the settlement.

Another high resistivity area in the survey grid is located in the north-central region of the survey grid. The area of interest corresponds to the high magnetic anomaly A21, while expanding its size in all directions. Nevertheless, the sampling resolution is not high enough to fully decipher the real shape of the anomaly. Another patch of relatively high resistance area is located to the south of A21, but without providing further information about its spatial characteristics. Finally, the low resistance area between the core of the settlement (A21) and the built enclosure (A3) suggests preferential avoidance of habitation/use, as the magnetic data have already suggested.

Soil Studies

Two transects perpendicular to each other were sampled across the site, targeting different positive magnetic anomalies interpreted as enclosures and other potential structural anomalies previously detected by geophysical means (Figure 25). The lines were sampled collecting soil at 2 depths: A (0.10-0.15m) and B (0.15-0.20m). A series of points targeting the above mentioned anomalies were augered until the feature/solid geology was reached. Most of the dich-like anomalies were augered up to 0.35-0.5m when fairly flat stone was reached (Figures 26 and 27). Two control samples were collected outside the site.

The mean values of the low frequency MS measurements along the different lines (Table 3) were fairly similar 1.32E-06 and 1.22E-6 (A samples) and between 1.21E-06 and 1.35E-06 (B samples). These in-site values were between 145%/160% higher than the values of the control (off-site) samples collected at the same A and B depths respectively. The P concentration in all the lines sampled was significantly enhanced (Table 3). Averaged P values of 453.22 ppm were obtained from the control samples and 1795.23 ppm from the in-site samples.

MEAN VALUES & % INCREASE (LINE SAMPLES, PERDIKA)							
Analysis		**Magnetic Susceptibility (χlf, $10^{-6}m^3kg^{-1}$)**				**Phosphate (ppm)**	
Depth	**Length (m)**	**N°**	**A (0.10-0.15m)**	**N°**	**B (0.15-0.20m)**	**N°**	**B (0.15-0.20m)**
LINE 1	158	35	1.32E-06	28	1.21E-06	27	1934.61
LINE 2	82	16	1.22E-06	16	1.35E-06	10	1655.86
Mean			**1.27E-06**		**1.28E-06**		**1795.23**
CONTROL 1		1	4.53E-07	1	4.03E-07		
CONTROL 2		1	5.85E-07	1	5.84E-07		
Mean			5.19E-07		4.93E-07		
% Increase			**144.47%**		**159.34%**		

Table 3: The table shows the mean values of the results of the low frequency MS (χ_{lf}) and P analyses (ppm=parts per millions) of the lines sampled at Perdika 2 at two depths (A & B) and the off-site control samples. The table also shows the total percentage increase in MS of the off-site/in-site samples.

Figure 24: Different views of the Perdika 2 site during the soil sampling: SE view of the field where Line 1 was sampled (top) and NW view of the sample line (bottom). The locations of the lines samples at Perdika 2 are detailed in **Error! Reference source not found.**.

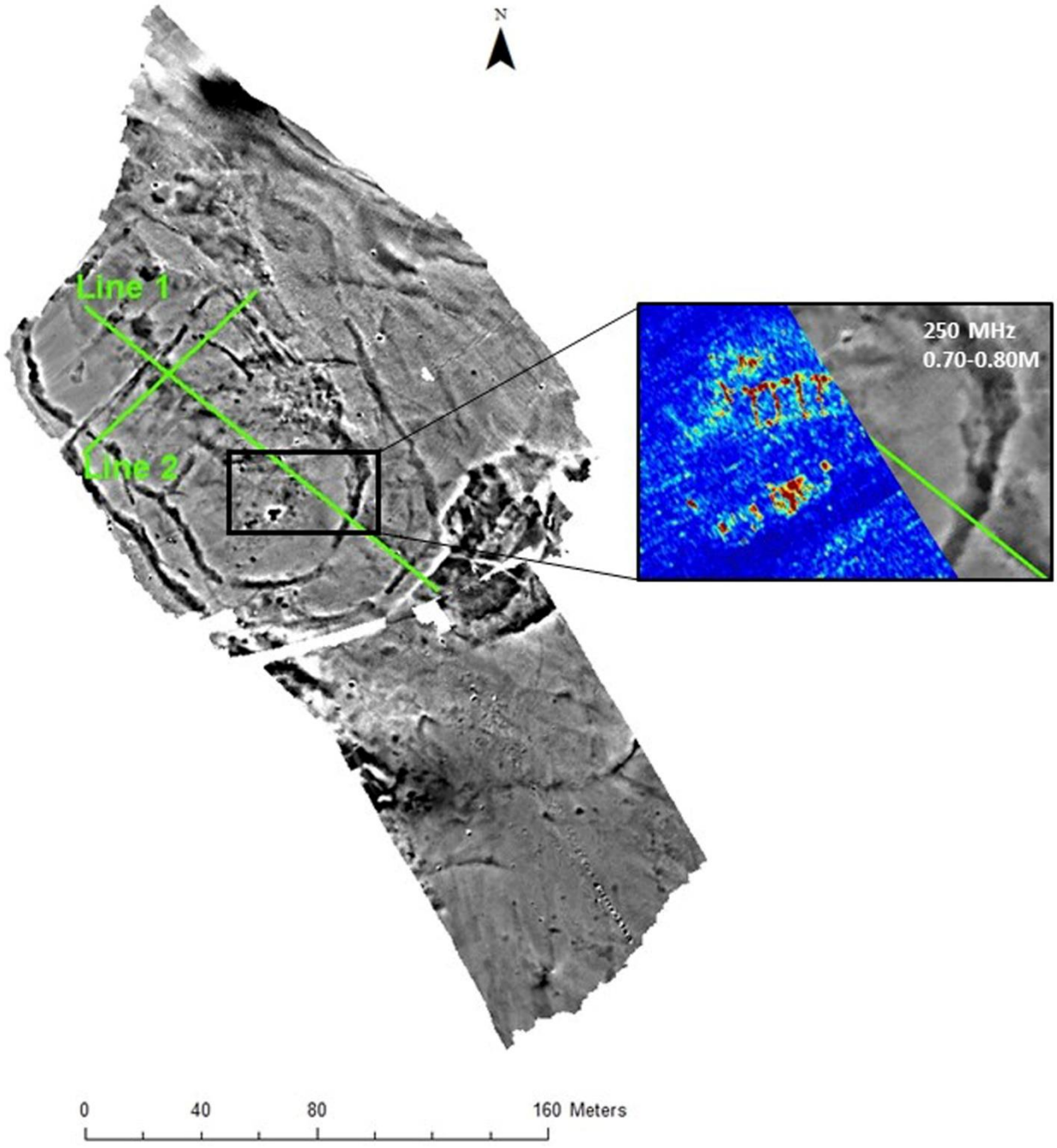

Figure 25: Location of the sampled lines (in green) in Perdika 2. The grey scale image shows the results of the magnetometer survey (positive magnetic anomalies are displayed in black and negative magnetic anomalies in white). The inset contains a detail of a time-slice (~0.70-0.80m depth) showing a series of possible structures with the GPR survey (250MHz central frequency antenna).

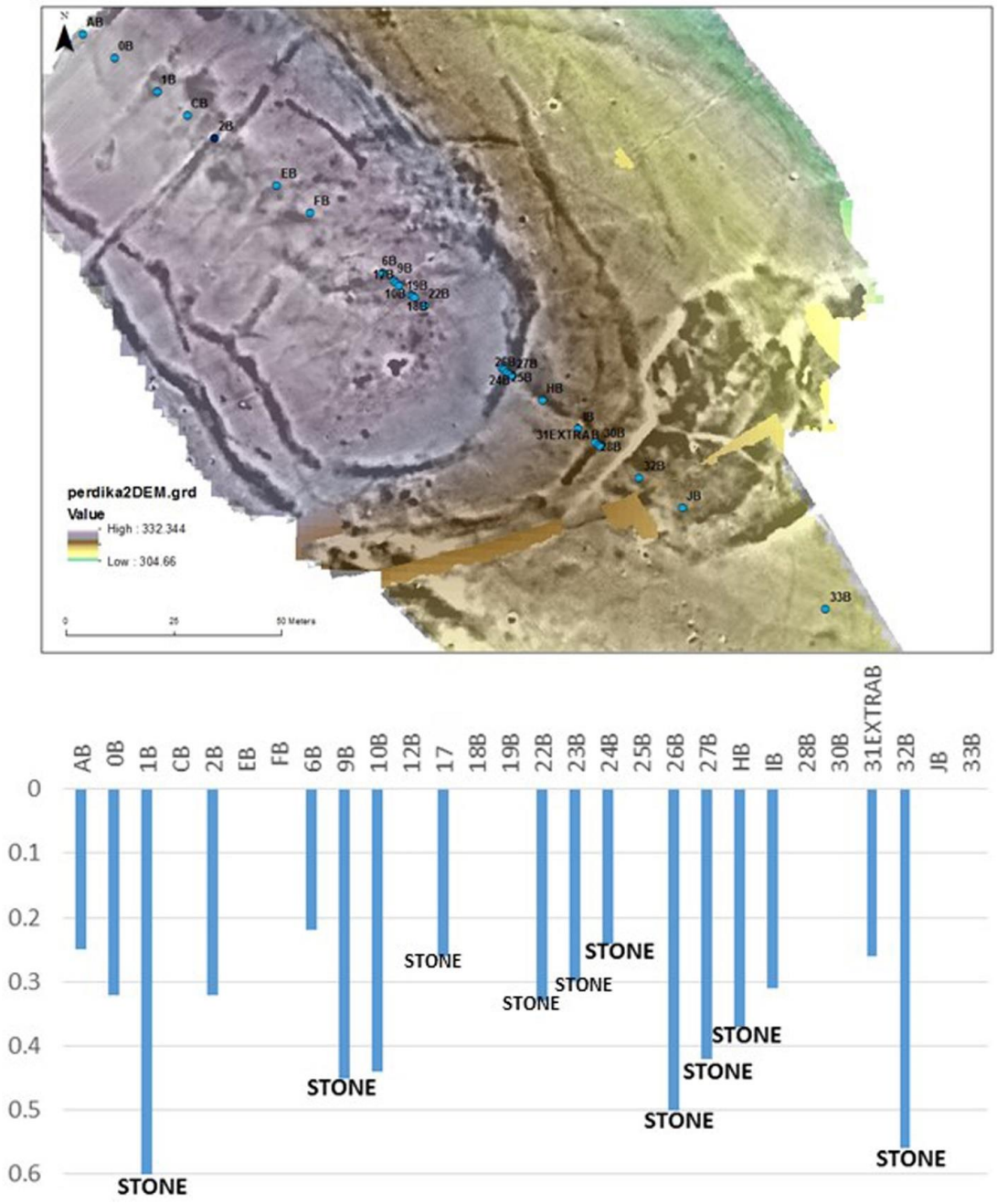

Figure 26: Location of the samples collected along Line 1 in Perdika 2 and the depths reached with the targeted 'auger' sampling. The grey scale image shows the results of the magnetometer survey (positive magnetic anomalies are displayed in black and negative magnetic anomalies in white). The image shows also the results of the digital elevation model (DEM) overlying the magnetometer results. The vertical axis in the graphs shows the depth from the surface in meters and the horizontal axis shows the code of the samples.

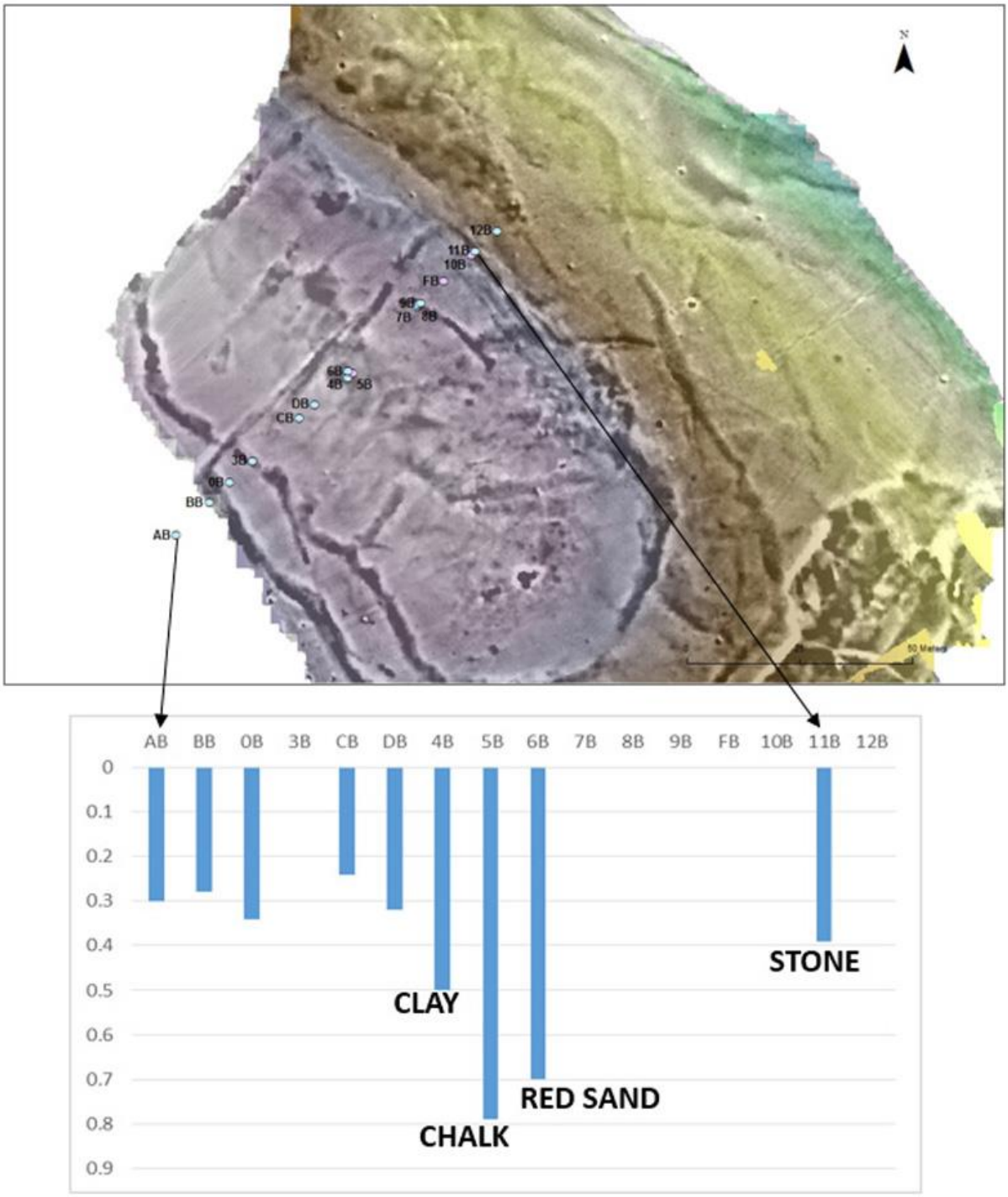

Figure 27: Location of the samples collected along Line 2 in Perdika 2 and the depths reached with the targeted 'auger' sampling. The grey scale image shows the results of the magnetometer survey (positive magnetic anomalies are displayed in black and negative magnetic anomalies in white). The image shows also the results of the digital elevation model (DEM) overlying the magnetometer results.

Line 1

Apart from some high MS values obtained at the location of linear positive magnetic anomalies (e.g. 3.07E-06 in Table 4), there were not particular areas with well-defined lateral MS enhancements. However, there was a fairly coherent area of lateral P enhancement in the middle of Line 1 and within the innermost enclosure (Figure 29). The results of the spearman correlation analysis (Figure 30) showed a positive and linear association between the MS and P results which was not that obvious in Figures 28 and 29.

The 'auger' samples generally did not shown any clear pattern and had similar MS and FD values, except Point 32 (Figure 28). This point showed some MS enhancement from 0.24m depth until stone was reached at 0.56m depth. Whist the FD values varied between 9-10% in the most of the samples, the samples from Point 32 ranged from 11-13%. This means that high percentage in SP grains are present in the samples collected at this areas, outside of the main enclosures revealing the presence of enhanced soil related to human activity or a possible burned soils here.

Line 2

The results showed some MS and P enhancement towards the northern most sampling points (Figures 31 and 32). Sample A (Table 6) gave high MS results despite been outside of the outermost enclosure. This sample was taken in a degraded area with very thin soils and a lot of vegetation, some of them burnt, which may be the reason for the relatively high MS and FD values.

The 'auger' samples showed rather lower values until reaching Point 5 and 6 which were take over a positive magnetic anomaly (Figure 31). The soils extracted with the auger at Point 4 (Table 7) were very clayey and moist which may explain the depleted MS values (e.g. presence of weakly magnetic minerals or reduction of iron oxides resulting from the higher water retention in heavy clay soils). The soil at Point 5 was fairly chalky and had light beige/reddish colour. This sample had the higher mean MS values with a peak (>2.25E-06 m^3kg^{-1}) at 0.64m depth. Point 6 sample had a MS peak (2.28E-06 m^3kg^{-1}) at 0.40m. The last auger sampled was Point 11. Stone was reached at 0.39m and a peak in MS (~2E-06 m^3kg^{-1}) was measured at 0.30m depth (Table 7)

LINE 1 (PERDIKA 2)							
Analysis	Magnetic Susceptibility						Phosphate
Depth	A (0.10-0.15m)			B (0.15-0.20m)			B (0.15-0.20m)
ID	χlf	χhf	FD (%)	χlf	χhf	FD (%)	(ppm)
A	1.10E-06	9.89E-07	10.33	1.09E-06	9.86E-07	9.98	986.11
0	6.02E-07	5.47E-07	9.16	6.34E-07	5.71E-07	10.00	745.29
1	1.68E-06	1.51E-06	10.32	1.54E-06	1.38E-06	9.93	2835.12
C	6.14E-07	5.52E-07	10.10	4.89E-07	4.40E-07	9.99	324.36
2	2.70E-06	2.41E-06	10.46	3.07E-06	2.75E-06	10.31	1962.99
D	3.14E-07	2.83E-07	9.87				
E	1.60E-06	1.43E-06	10.27	1.74E-06	1.56E-06	9.99	3515.77
F	9.07E-07	8.18E-07	9.83	7.92E-07	7.15E-07	9.80	1072.89
3	1.81E-06	1.63E-06	10.13				
6	1.98E-06	1.77E-06	10.88	1.82E-06	1.62E-06	10.61	3326.1
7	1.65E-06	1.48E-06	10.32				
8	1.93E-06	1.73E-06	10.11				
9	1.82E-06	1.63E-06	10.32	1.45E-06	1.30E-06	10.42	2704.62
10	1.88E-06	1.69E-06	10.20	1.37E-06	1.23E-06	10.45	2809.94
12	1.78E-06	1.60E-06	10.31	1.69E-06	1.51E-06	10.40	1766
17	1.25E-06	1.12E-06	10.00	1.13E-06	1.01E-06	10.35	2222.81
18	1.59E-06	1.42E-06	10.35	1.41E-06	1.26E-06	10.83	3188.3
19	1.05E-06	9.48E-07	10.03	1.02E-06	9.14E-07	10.15	2613.35
20	1.07E-06	9.56E-07	10.23				
21	1.32E-06	1.19E-06	10.42				
22	0.000000961	8.68E-07	9.6435	9.091E-07	8.16E-07	10.2755	3225.39
23	1.1764E-06	1.05E-06	10.3487	1.0907E-06	9.82E-07	9.9954	3074.32
24	1.2363E-06	1.12E-06	9.441	1.2974E-06	1.16E-06	10.7928	2287.9
25	1.1396E-06	1.02E-06	10.4415	1.2747E-06	1.14E-06	10.5863	2009.35
26	0.000001107	1.01E-06	8.6125	1.2551E-06	1.14E-06	9.0848	3168.14
27	1.0666E-06	9.55E-07	10.4909	1.1337E-06	1.02E-06	9.8036	2229.52
H	6.493E-07	5.8E-07	10.6591	6.254E-07	5.64E-07	9.8693	1752.44
I	1.0271E-06	9.18E-07	10.5857	7.654E-07	6.82E-07	10.8603	526.09
28	1.4252E-06	1.27E-06	10.5588	0.000001283	1.14E-06	10.7574	1267.72
29	0.000001552	1.39E-06	10.6005				
30	1.5784E-06	1.41E-06	10.6919	1.6729E-06	1.49E-06	10.7283	1485.13
31	1.7113E-06	1.53E-06	10.7246	5.531E-07	4.95E-07	10.5827	410.21
32	1.2153E-06	1.08E-06	11.0349	1.4994E-06	1.32E-06	11.8314	823.38
J	6.034E-07	5.36E-07	11.1955	5.454E-07	4.89E-07	10.3206	313.51
33	1.0498E-06	9.39E-07	10.5342	6.889E-07	6.19E-07	10.2063	573.87
MIN	**3.14E-07**	**2.83E-07**	**8.61**	**4.89E-07**	**4.40E-07**	**9.08**	**313.51**
MAX	**2.70E-06**	**2.41E-06**	**11.20**	**3.07E-06**	**2.75E-06**	**11.83**	**3515.77**
MEAN	**1.32E-06**	**1.18E-06**	**10.26**	**1.21E-06**	**1.08E-06**	**10.32**	**1900.74**
S.D.	**4.91E-07**	**4.39E-07**	**0.50**	**5.35E-07**	**4.79E-07**	**0.50**	**1050.13**
C.V.	**37.27**	**37.15**	**4.87**	**44.32**	**44.25**	**4.82**	**55.25**

Table 4: Results of the MS and P analyses of the soil sampled in Line 1 at Perdika 2 at two different depths (A & B). The abbreviations stand for: low frequency MS (χ_{lf}), high frequency MS (χ_{hf}), frequency dependent percentage (fd%) and parts per million (ppm). The table also shows the minimum (MIN) and maximum (MAX) values, as well as the mean, standard deviation (S.D.) and coefficient of variation (C.V.) of the measurements

PROFILE SAMPLES FROM LINE 1 (PERDIKA 2)

Magnetic Susceptibility

POINT 6				POINT 9				POINT 10				POINT 22				POINT 23				POINT 26				POINT 27			
Depth	χlf	χhf	FD (%)	DEPTH	χlf	χhf	FD (%)	DEPTH	χlf	χhf	FD (%)	DEPTH	χlf	χhf	FD (%)	DEPTH	χlf	χhf	FD (%)	DEPTH	χlf	χhf	FD (%)	DEPTH	χlf	χhf	FD (%)
0.22-0.26	1.73E-06	1.60E-06	7.85	0.10-0.16	1.82E-06	1.63E-06	10.32	0.10-0.12	1.88E-06	1.69E-06	10.20	0.12-0.16	9.61E-07	8.68E-07	9.64	0.12-0.16	1.18E-06	1.05E-06	10.35	0.12-0.16	1.11E-06	1.01E-06	8.61	0.12-0.16	1.07E-06	9.55E-07	10.49
0.26-0.31	1.73E-06	1.61E-06	6.72	0.16-0.19	1.45E-06	1.30E-06	10.42	0.12-0.15	1.37E-06	1.23E-06	10.45	0.16-0.20	9.09E-07	8.16E-07	10.28	0.16-0.20	1.09E-06	9.82E-07	10.00	0.16-0.22	1.26E-06	1.14E-06	9.08	0.16-0.22	1.13E-06	1.02E-06	9.80
0.31-0.36	1.71E-06	1.58E-06	7.50	0.19-0.23	1.31E-06	1.17E-06	10.55	0.15-0.23	1.27E-06	1.15E-06	10.02	0.20-0.24	8.30E-07	7.41E-07	10.72	0.20-0.25	9.63E-07	8.63E-07	10.33	0.22-0.26	1.25E-06	1.13E-06	9.53	0.22-0.31	1.68E-06	1.51E-06	9.88
0.36-0.42	1.64E-06	1.53E-06	6.70	0.23-0.28	1.19E-06	1.07E-06	9.94	0.23-0.28	1.18E-06	1.06E-06	10.35	0.24-0.28	8.98E-07	8.06E-07	10.30	0.25-0.30	1.02E-06	9.16E-07	10.22	0.26-0.30	1.18E-06	1.07E-06	9.80	0.31-0.35	1.87E-06	1.69E-06	9.73
0.42-0.48	1.70E-06	1.58E-06	7.42	0.28-0.30	1.18E-06	1.06E-06	10.06	0.28-0.30	1.21E-06	1.08E-06	10.66	0.28-0.33	8.52E-07	7.69E-07	9.77					0.30-0.36	1.17E-06	1.06E-06	9.70	0.35-0.42	1.55E-06	1.40E-06	9.49
0.48-0.56	1.79E-06	1.66E-06	7.23	0.30-0.34	1.33E-06	1.19E-06	10.47	0.30-0.36	1.11E-06	1.00E-06	10.16									0.36-0.39	1.07E-06	9.64E-07	9.53				
0.56-0.62	1.79E-06	1.67E-06	6.60	0.34-0.40	1.05E-06	9.47E-07	9.88	0.36-0.40	1.03E-06	9.27E-07	10.02									0.39-0.48	9.69E-07	8.79E-07	9.26				
0.62-0.68	1.56E-06	1.46E-06	6.50	0.40-0.45	1.18E-06	1.06E-06	10.34	0.40-0.44	1.04E-06	9.34E-07	9.74									0.48-0.50	1.02E-06	9.20E-07	9.64				
0.68-0.79	1.70E-06	1.59E-06	6.72					0.44-0.52	1.02E-06	9.17E-07	9.93																
0.79-0.9	1.67E-06	1.55E-06	7.06																								
0.9-0.96	1.66E-06	1.53E-06	7.69																								
0.97-1.06	1.532E-06	1.42E-06	7.52																								
MIN	**1.53E-06**	**1.42E-06**	**6.50**		**1.05E-06**	**9.47E-07**	**9.88**		**1.02E-06**	**9.17E-07**	**9.74**		**8.30E-07**	**7.41E-07**	**9.64**		**9.63E-07**	**8.63E-07**	**10.00**		**9.69E-07**	**8.79E-07**	**8.61**	**MIN**	**1.07E-06**	**9.55E-07**	**9.49**
MAX	**1.79E-06**	**1.67E-06**	**7.85**		**1.82E-06**	**1.63E-06**	**10.55**		**1.88E-06**	**1.69E-06**	**10.66**		**9.61E-07**	**8.68E-07**	**10.72**		**1.18E-06**	**1.05E-06**	**10.35**		**1.26E-06**	**1.14E-06**	**9.80**	**MAX**	**1.87E-06**	**1.69E-06**	**10.49**
MEAN	**1.68E-06**	**1.56E-06**	**7.03**		**1.31E-06**	**1.18E-06**	**10.25**		**1.23E-06**	**1.11E-06**	**10.17**		**8.90E-07**	**8.00E-07**	**10.14**		**1.06E-06**	**9.54E-07**	**10.22**		**1.13E-06**	**1.02E-06**	**9.39**	**MEAN**	**1.46E-06**	**1.32E-06**	**9.88**
S.D.	**7.90E-08**	**7.38E-08**	**0.47**		**2.3802E-07**	**2.12E-07**	**0.25**		**2.6983E-07**	**2.41E-07**	**0.28**		**5.12E-08**	**4.84E-08**	**0.44**		**9.22E-08**	**8.28E-08**	**0.16**		**1.06E-07**	**9.56E-08**	**0.39**	**S.D.**	**3.5E-07**	**3.18E-07**	**0.37**
C.V.	**4.69**	**4.72**	**6.70**		**18.14**	**18.01**	**2.47**		**21.86**	**21.77**	**2.79**		**5.75**	**6.05**	**4.30**		**8.68**	**8.68**	**1.59**		**9.37**	**9.36**	**4.17**	**C.V.**	**23.94**	**24.15**	**3.78**

POINT H				POINT I				POINT 31				POINT 32				CONTROL 1				CONTROL 2			
DEPTH	χlf	χhf	FD (%)	DEPTH	χlf	χhf	FD (%)	DEPTH	χlf	χhf	FD (%)	DEPTH	χlf	χhf	FD (%)	DEPTH	χlf	χhf	FD (%)	DEPTH	χlf	χhf	FD (%)
0.12-0.17	6.49E-07	5.80E-07	10.66	0.12-0.17	1.03E-06	9.18E-07	10.59	0.12-0.20	1.71E-06	1.53E-06	10.72	0.11-0.16	1.22E-06	1.08E-06	11.03	0.15-0.18	4.53E-07	4.09E-07	9.69	0.10-0.13	5.82E-07	5.24E-07	9.94
0.17-0.21	6.25E-07	5.64E-07	9.87	0.17-0.23	7.65E-07	6.82E-07	10.86	0.12-0.15	1.07E-06	9.60E-07	10.55	0.16-0.20	1.50E-06	1.32E-06	11.83	0.18-0.24	4.03E-07	3.62E-07	10.12	0.13-0.17	5.87E-07	5.32E-07	9.44
0.21-0.31	4.95E-07	4.47E-07	9.82	0.23-0.27	7.68E-07	6.89E-07	10.29	0.15-0.21	5.53E-07	4.95E-07	10.58	0.20-0.24	1.74E-06	1.52E-06	12.63	0.24-0.30	3.38E-07	3.08E-07	8.71	0.17-0.21	5.80E-07	5.24E-07	9.67
0.31-0.37	3.76E-07	3.42E-07	9.16	0.27-0.31	7.21E-07	6.47E-07	10.25	0.21-0.26	4.88E-07	4.36E-07	10.51	0.24-0.27	2.10E-06	1.83E-06	13.04	0.30-0.38	3.27E-07	2.96E-07	9.29	0.21-0.28	5.70E-07	5.17E-07	9.27
												0.27-0.31	2.17E-06	1.90E-06	12.71	0.38-0.50	3.76E-07	3.40E-07	9.60	0.28-0.30	5.99E-07	5.43E-07	9.32
												0.31-0.34	2.04E-06	1.77E-06	12.96	0.50-0.58	4.18E-07	3.80E-07	9.11				
												0.34-0.36	2.04E-06	1.77E-06	12.94								
												0.36-0.39	2.13E-06	1.86E-06	12.91								
												0.41-0.45	2.15E-06	1.87E-06	13.09								
												0.45-0.48	1.95E-06	1.69E-06	13.20								
												0.48-0.52	1.80E-06	1.57E-06	12.95								
												0.52-0.56	1.92E-06	1.68E-06	12.55								
MIN	**3.76E-07**	**3.42E-07**	**9.16**	**MIN**	**7.21E-07**	**6.47E-07**	**10.25**	**MIN**	**4.88E-07**	**4.36E-07**	**10.51**	**MIN**	**1.22E-06**	**1.08E-06**	**11.03**	**MIN**	**3.27E-07**	**2.96E-07**	**8.71**	**MIN**	**5.70E-07**	**5.17E-07**	**9.27**
MAX	**6.49E-07**	**5.80E-07**	**10.66**	**MAX**	**1.03E-06**	**9.18E-07**	**10.86**	**MAX**	**1.71E-06**	**1.53E-06**	**10.72**	**MAX**	**2.17E-06**	**1.90E-06**	**13.20**	**MAX**	**4.53E-07**	**4.09E-07**	**10.12**	**MAX**	**5.99E-07**	**5.43E-07**	**9.94**
MEAN	**5.37E-07**	**4.83E-07**	**9.88**	**MEAN**	**8.20E-07**	**7.34E-07**	**10.50**	**MEAN**	**9.56E-07**	**8.55E-07**	**10.59**	**MEAN**	**1.90E-06**	**1.65E-06**	**12.65**	**MEAN**	**3.86E-07**	**3.49E-07**	**9.42**	**MEAN**	**5.84E-07**	**5.28E-07**	**9.53**
S.D.	**1.266E-07**	**1.11E-07**	**0.61**	**S.D.**	**1.3957E-07**	**1.24E-07**	**0.28**	**S.D.**	**5.6741E-07**	**5.06E-07**	**0.09**	**S.D.**	**2.91E-07**	**2.46E-07**	**0.62**	**S.D.**	**4.84E-08**	**4.3E-08**	**0.49**	**S.D.**	**1.09E-08**	**1.01E-08**	**0.28**
C.V.	**23.60**	**23.08**	**6.21**	**C.V.**	**17.01**	**16.92**	**2.71**	**C.V.**	**59.34**	**59.23**	**0.89**	**C.V.**	**15.36**	**14.89**	**4.93**	**C.V.**	**12.55**	**12.31**	**5.25**	**C.V.**	**1.87**	**1.92**	**2.89**

Table 5: Results of the MS analysis of the auger samples from Line 1 and the off-site controls collected at Perdika 2. The abbreviations stand for: low frequency MS (χ_{lf}), high frequency MS (χ_{hf}), frequency dependent percentage (fd%) and parts per million (ppm). The table also shows the minimum (MIN) and maximum (MAX) values, as well as the mean, standard deviation (S.D.) and coefficient of variation (C.V.) of the measurements.

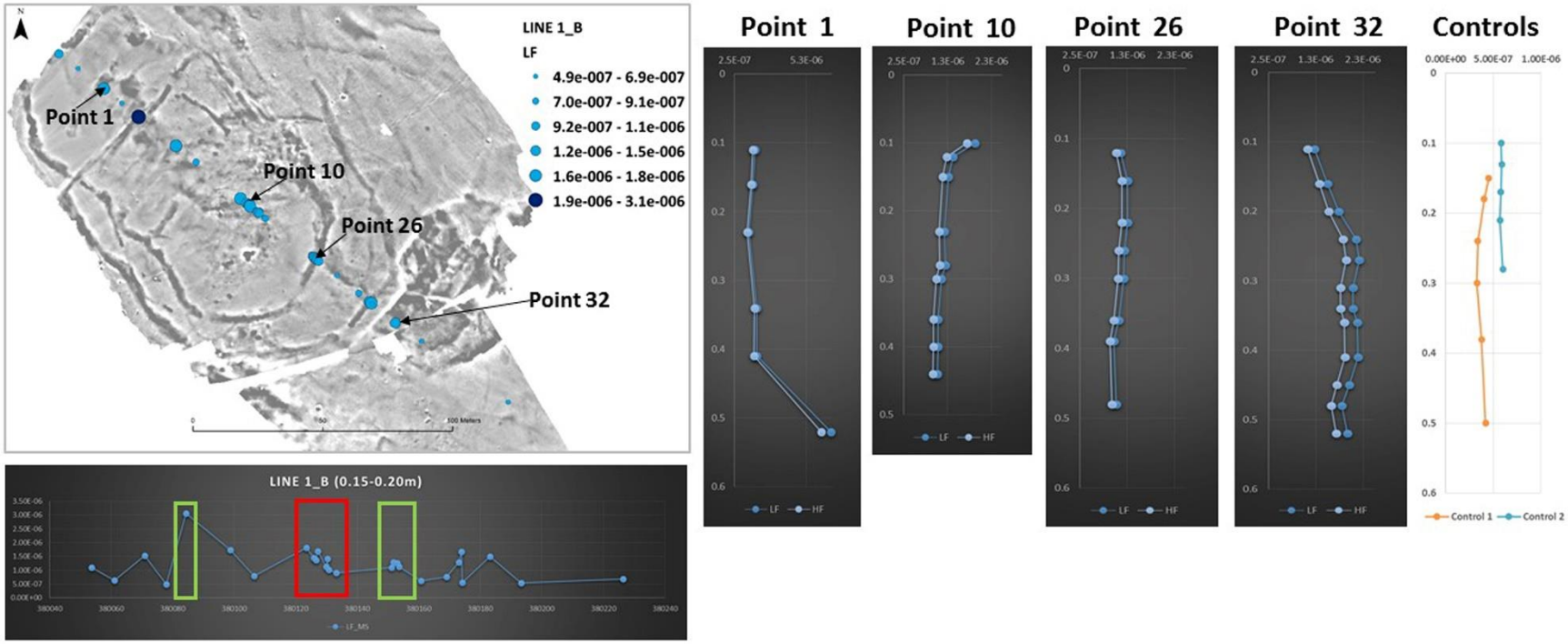

Figure 28: Bubble plot and graph showing the lateral MS distribution along Line 1_B (Perdika2). In the graph, the location of the targeted enclosures (in green) and structures (only detected with the GPR survey) are indicated in green and red respectively. The results of the 'auger' samples at Point 5 and control samples are also shown.

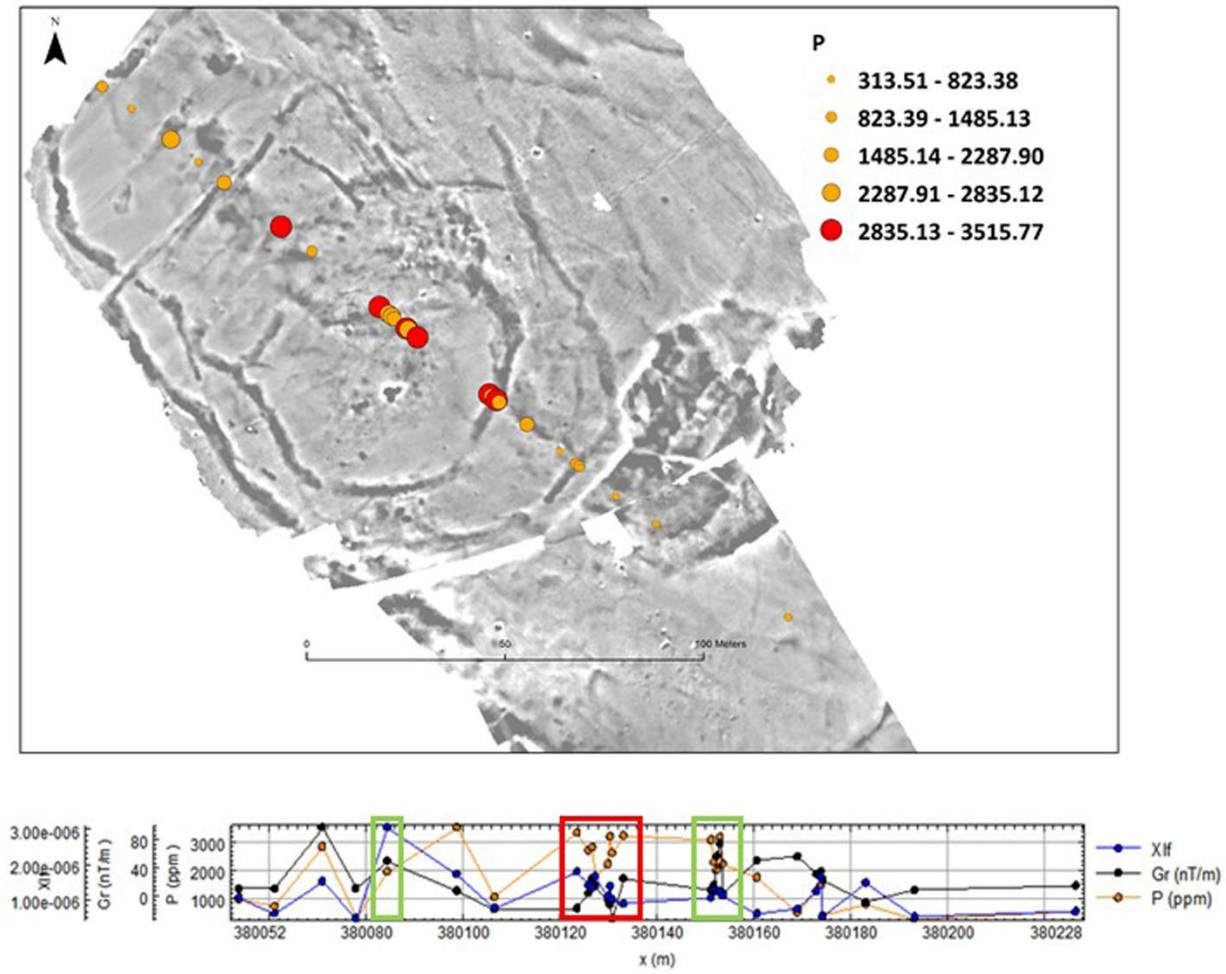

Figure 29: Bubble plot (above) showing the lateral P distribution along Line 1_B (Perdika2). The graph (below) shows the lateral variation of the magnetic intensity gradient (Gr), MS (X_{lf}) and P content. In the graph, the location of the targeted enclosures (in green) and structures (only detected with the GPR survey) are indicated in green and red respectively.

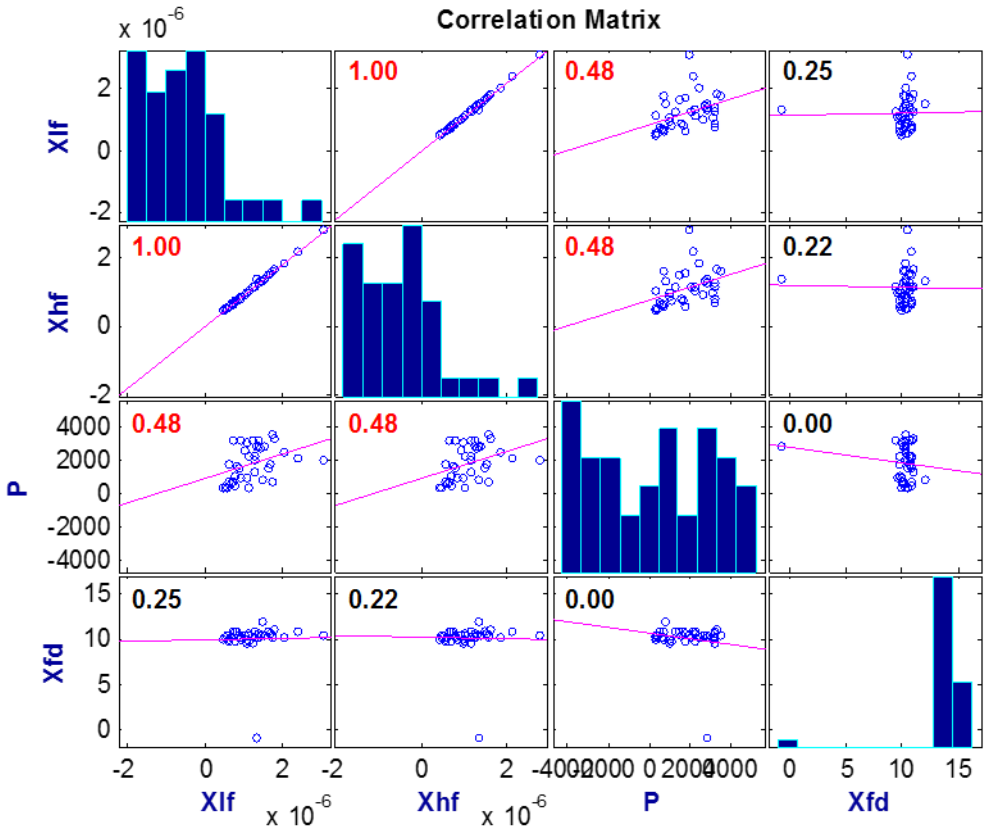

Figure 30: Results of the Spearman correlation (Line1_B, Perdika2)

LINE 2 (PERDIKA 2)							
Analysis	**Magnetic Susceptibility**						**Phosphate**
Depth	**A (0.10-0.15m)**			**B (0.15-0.20m)**			**B (0.15-0.20m)**
ID	**χlf**	**χhf**	**FD (%)**	**χlf**	**χhf**	**FD (%)**	**(ppm)**
A	9.68E-07	8.69E-07	10.20	1.77E-06	1.59E-06	10.28	720.29
B	6.62E-07	6.04E-07	8.85	6.80E-07	6.17E-07	9.22	
0	5.02E-07		9.73	9.25E-07	8.33E-07	10.03	979.27
2	9.00E-07	5.56E-07	0.00				
3	1.03E-06	9.34E-07	9.53	1.07E-06	9.68E-07	9.89	
C	7.86E-07	7.05E-07	10.30	9.23E-07	8.27E-07	10.44	
D	1.07E-06	9.56E-07	10.20	7.13E-07	6.36E-07	10.71	736.48
4	2.64E-06	2.35E-06	10.80	9.47E-07	8.49E-07	10.34	
5	2.64E-06	2.36E-06	10.70	2.53E-06	2.26E-06	10.70	
6	7.01E-07	6.36E-07	9.29	1.16E-06	1.04E-06	10.17	315.63
7	9.66E-07	8.68E-07	10.10	2.05E-06	1.84E-06	10.46	2452.22
8	2.49E-07	2.26E-07	9.16	7.35E-07	6.55E-07	10.80	3164.42
9				1.35E-06	1.36E-06		
F	6.17E-07	5.57E-07	9.70	2.40E-06	2.14E-06	10.92	2856.88
10	1.51E-06	1.51E-06	0.00	2.62E-06	2.34E-06	10.98	2144.68
11	2.74E-06	2.45E-06	10.80	8.75E-07	7.84E-07	10.34	1561.98
12	2.25E-06	2.01E-06	10.70	8.39E-07	7.48E-07	10.89	1626.72
MIN	**2.49E-07**	**2.26E-07**	**0.00**	**6.80E-07**	**6.17E-07**	**9.22**	**315.63**
MAX	**2.74E-06**	**2.45E-06**	**10.80**	**2.62E-06**	**2.34E-06**	**10.98**	**3164.42**
MEAN	**1.26E-06**	**1.17E-06**	**8.75**	**1.35E-06**	**1.22E-06**	**10.41**	**1655.86**
S.D.	**8.30E-07**	**7.57E-07**	**3.47**	**6.91E-07**	**6.16E-07**	**0.47**	**976.13**
C.V.	**65.65**	**64.53**	**39.63**	**51.20**	**50.60**	**4.49**	**58.95**

Table 6: Results of the MS and P analyses of the soil sampled in Line 2 at Perdika 2 at two different depths (A & B). The abbreviations stand for: low frequency MS (χ_{lf}), high frequency MS (χ_{hf}), frequency dependent percentage (fd%) and parts per million (ppm). The table also shows the minimum (MIN) and maximum (MAX) values, as well as the mean, standard deviation (S.D.) and coefficient of variation (C.V.) of the measurements

PROFILE SAMPLES FROM LINE 2 (PERDIKA 2)																
Magnetic Susceptibility																
POINT A				POINT B				POINT 0				POINT C				POINT D			
Depth	χlf	χhf	FD (%)	DEPTH	χlf	χhf	FD (%)	DEPTH	χlf	χhf	FD (%)	DEPTH	χlf	χhf	FD (%)	DEPTH	χlf	χhf	FD (%)
0.11-0.16	9.68E-07	8.69E-07	10.24	0.11-0.15	6.62E-07	6.04E-07	8.85	0.11-0.16	5.56E-07	5.02E-07	9.73	0.11-0.16	7.86E-07	7.05E-07	10.25	0.11-0.16	1.07E-06	9.56E-07	10.25
0.16-0.20	1.77E-06	1.59E-06	10.28	0.15-0.23	6.80E-07	6.17E-07	9.22	0.16-0.21	9.25E-07	8.33E-07	10.03	0.16-0.22	9.23E-07	8.27E-07	10.44	0.16-0.20	7.13E-07	6.36E-07	10.71
0.20-0.24	1.95E-06	1.75E-06	10.33	0.23-0.28	9.74E-07	8.77E-07	9.99	0.21-0.26	9.69E-07	8.75E-07	9.77	0.22-0.24	6.63E-07	6.05E-07	8.71	0.20-0.26	7.31E-07	6.60E-07	9.73
0.24-0.28	2.27E-06	2.03E-06	10.69					0.26-0.30	1.13E-06	1.03E-06	9.25					0.26-0.32	7.12E-07	6.47E-07	9.08
0.24-0.30	2.12E-06	1.89E-06	10.68					0.30-0.34	6.96E-07	6.31E-07	9.41								
MIN	**9.68E-07**	**8.69E-07**	**10.24**		**6.62E-07**	**6.04E-07**	**8.85**		**5.56E-07**	**5.02E-07**	**9.25**		**6.63E-07**	**6.05E-07**	**8.71**		**7.12E-07**	**6.36E-07**	**9.08**
MAX	**2.27E-06**	**2.03E-06**	**10.69**		**9.74E-07**	**8.77E-07**	**9.99**		**1.13E-06**	**1.03E-06**	**10.03**		**9.23E-07**	**8.27E-07**	**10.44**		**1.07E-06**	**9.56E-07**	**10.71**
MEAN	**1.82E-06**	**1.63E-06**	**10.44**		**7.72E-07**	**6.99E-07**	**9.35**		**8.56E-07**	**7.73E-07**	**9.64**		**7.91E-07**	**7.12E-07**	**9.80**		**8.05E-07**	**7.25E-07**	**9.94**
S.D.	**5.10E-07**	**4.54E-07**	**0.22**		**1.7544E-07**	**1.54E-07**	**0.58**		**2.287E-07**	**2.07E-07**	**0.31**		**1.3E-07**	**1.11E-07**	**0.95**		**1.74E-07**	**1.55E-07**	**0.70**
C.V.	**28.07**	**27.91**	**2.13**		**22.72**	**22.04**	**6.24**		**26.73**	**26.83**	**3.19**		**16.43**	**15.55**	**9.69**		**21.58**	**21.32**	**7.06**

POINT 4				POINT 5				POINT 6				POINT 11			
DEPTH	χlf	χhf	FD (%)	DEPTH	χlf	χhf	FD (%)	DEPTH	χlf	χhf	FD (%)	DEPTH	χlf	χhf	FD (%)
0.12-0.18	8.47E-07	7.61E-07	10.23	0.11-0.15	8.37E-07	7.49E-07	10.45	0.12-0.17	5.52E-07	4.97E-07	10.05	0.12-0.20	2.53E-06	2.26E-06	10.70
0.18-0.23	CLAY			0.18-0.25	7.48E-07	6.73E-07	10.01	0.17-0.22	4.69E-07	4.26E-07	9.20	0.20-0.25	2.62E-06	2.34E-06	10.98
0.23-0.28				0.32-0.40	2.49E-07	2.26E-07	9.16	0.27-0.31	7.81E-07	7.02E-07	10.20	0.30-0.34	2.64E-06	2.36E-06	10.75
0.28-0.36	7.35E-07	6.55E-07	10.80	0.40-0.49	2.70E-07	2.40E-07	11.20	0.30-0.32	9.47E-07	8.49E-07	10.34	0.34-0.39	2.65E-06	2.36E-06	10.89
0.36-0.44	2.08E-07	1.86E-07	10.58	0.49-0.55	1.09E-06	9.79E-07	10.25	0.32-0.40	8.69E-07	7.82E-07	10.02				
				0.55-0.64	1.14E-06	1.02E-06	10.11	0.40-0.48	9.66E-07	8.68E-07	10.13				
				0.64-0.74	1.16E-06	1.04E-06	10.17	0.48-0.56	7.01E-07	6.36E-07	9.29				
				0.74-0.79	5.18E-07	4.62E-07	10.77	0.56-0.64	9.19E-07	8.36E-07	9.08				
								0.64-0.70	6.17E-07	5.57E-07	9.70				
MIN	**2.08E-07**	**1.86E-07**	**10.23**	**MIN**	**2.49E-07**	**2.26E-07**	**9.16**	**MIN**	**4.69E-07**	**4.26E-07**	**9.08**	**MIN**	**2.53E-06**	**2.26E-06**	**10.70**
MAX	**8.47E-07**	**7.61E-07**	**10.80**	**MAX**	**1.16E-06**	**1.04E-06**	**11.20**	**MAX**	**9.66E-07**	**8.68E-07**	**10.34**	**MAX**	**2.65E-06**	**2.36E-06**	**10.98**
MEAN	**5.97E-07**	**5.34E-07**	**10.54**	**MEAN**	**7.51E-07**	**6.74E-07**	**10.27**	**MEAN**	**7.58E-07**	**6.84E-07**	**9.78**	**MEAN**	**2.61E-06**	**2.33E-06**	**10.83**
S.D.	**4.0812E-07**	**3.06E-07**	**0.29**	**S.D.**	**3.7341E-07**	**3.36E-07**	**0.59**	**S.D.**	**1.8255E-07**	**1.64E-07**	**0.48**	**S.D.**	**5.3E-08**	**4.55E-08**	**0.13**
C.V.	**68.40**	**57.25**	**2.71**	**C.V.**	**49.71**	**49.79**	**5.79**	**C.V.**	**24.09**	**23.93**	**4.86**	**C.V.**	**2.03**	**1.95**	**1.18**

Table 7: Results of the MS analysis of the auger samples from Line 2 and the off-site controls collected at Perdika 2. The abbreviations stand for: low frequency MS (χ_{lf}), high frequency MS (χ_{hf}), frequency dependent percentage (fd%) and parts per million (ppm). The table also shows the minimum (MIN) and maximum (MAX) values, as well as the mean, standard deviation (S.D.) and coefficient of variation (C.V.) of the measurements.

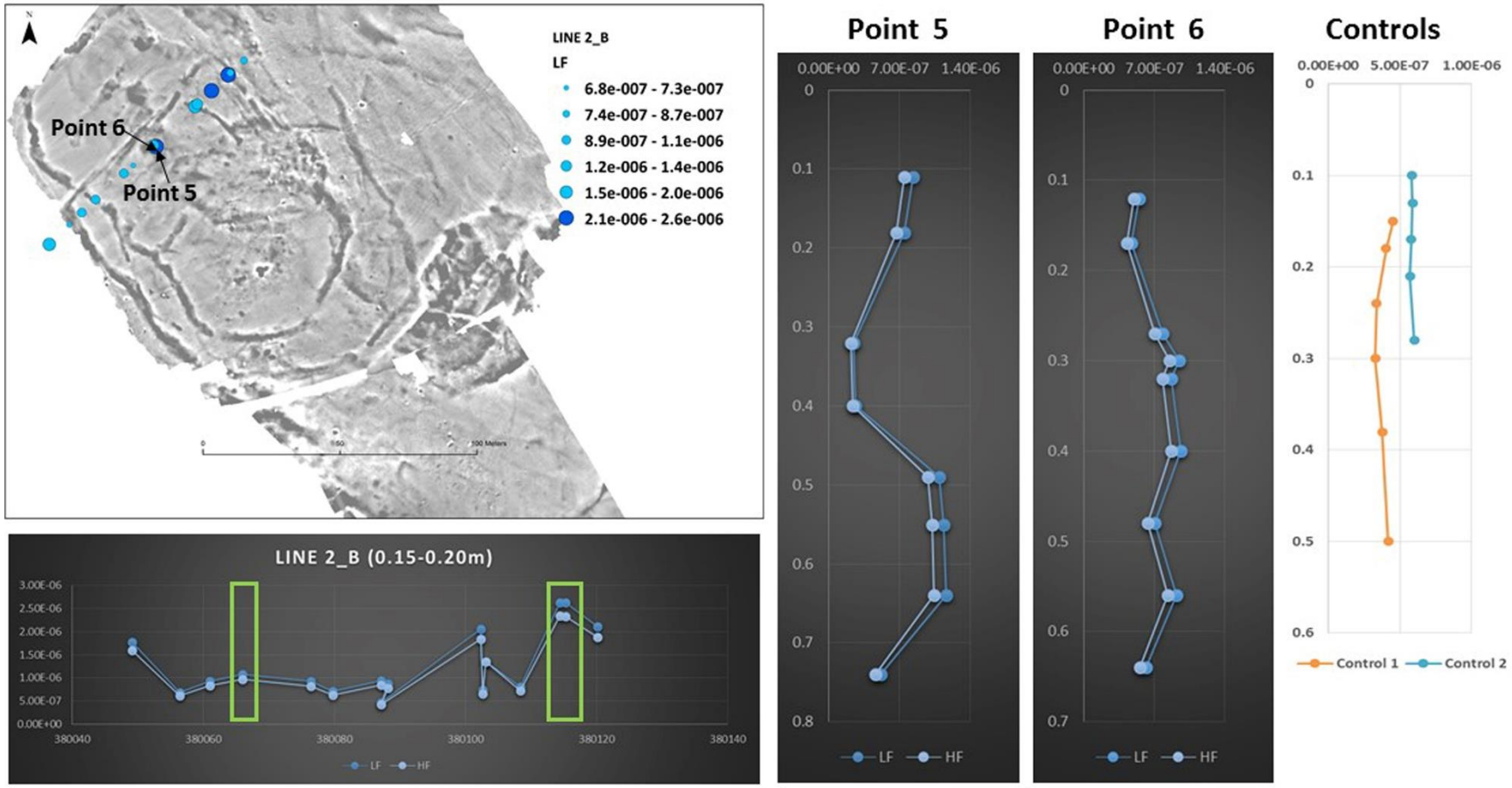

Figure 31: Bubble plot and graph showing the lateral MS distribution along Line 2_B (Perdika2). In the graph, the locations of the targeted enclosures (in green) are indicated in green and red respectively. The results of the 'auger' samples at Point 5, 6 and control samples are also shown.

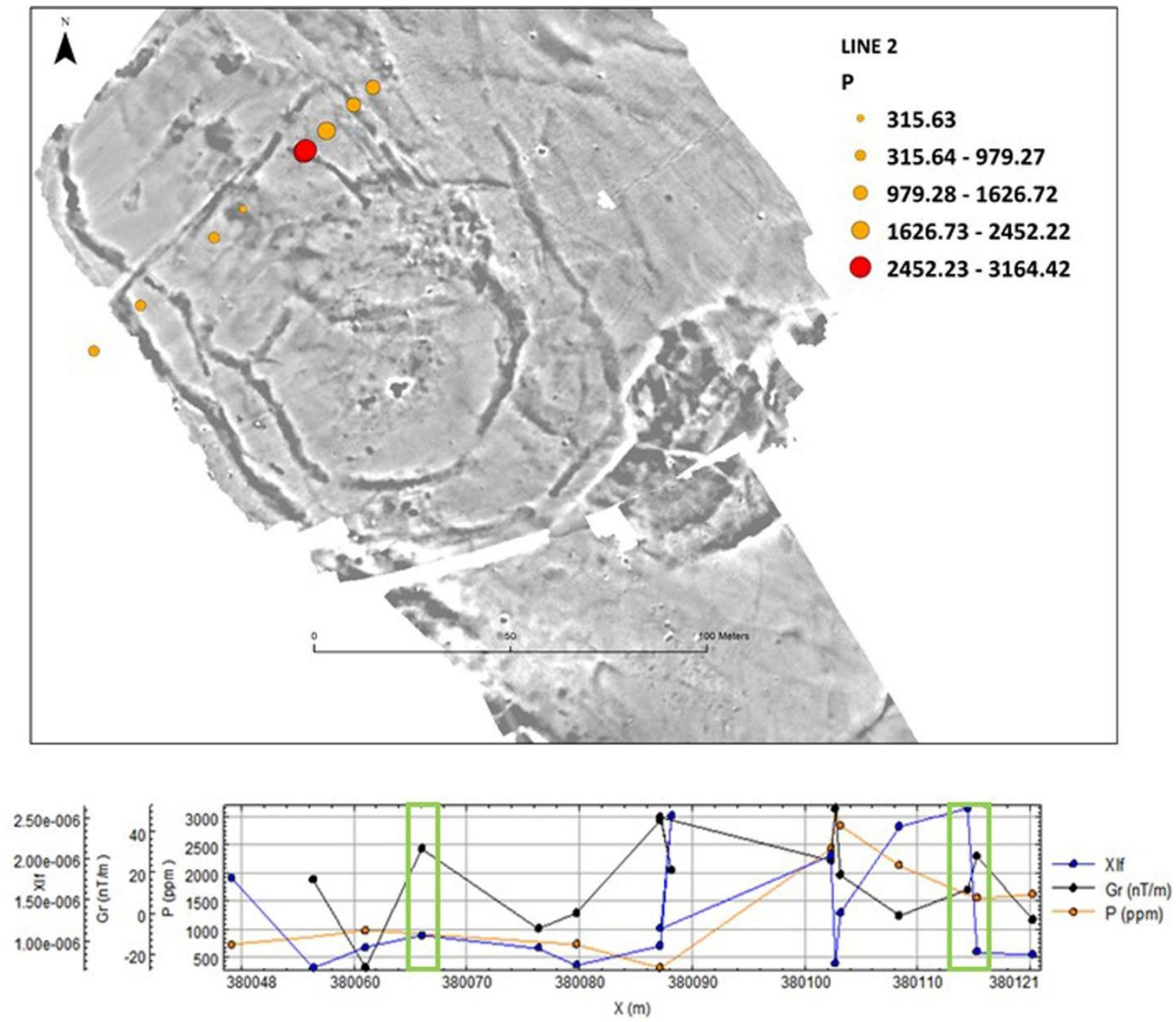

Figure 32: Bubble plot (above) showing the lateral P distribution along Line 2_B (Perdika2). The graph (below) shows the lateral variation of the magnetic intensity gradient (Gr), MS (X_{lf}) and P content. In the graph, the locations of the targeted enclosures are indicated in green and red respectively.

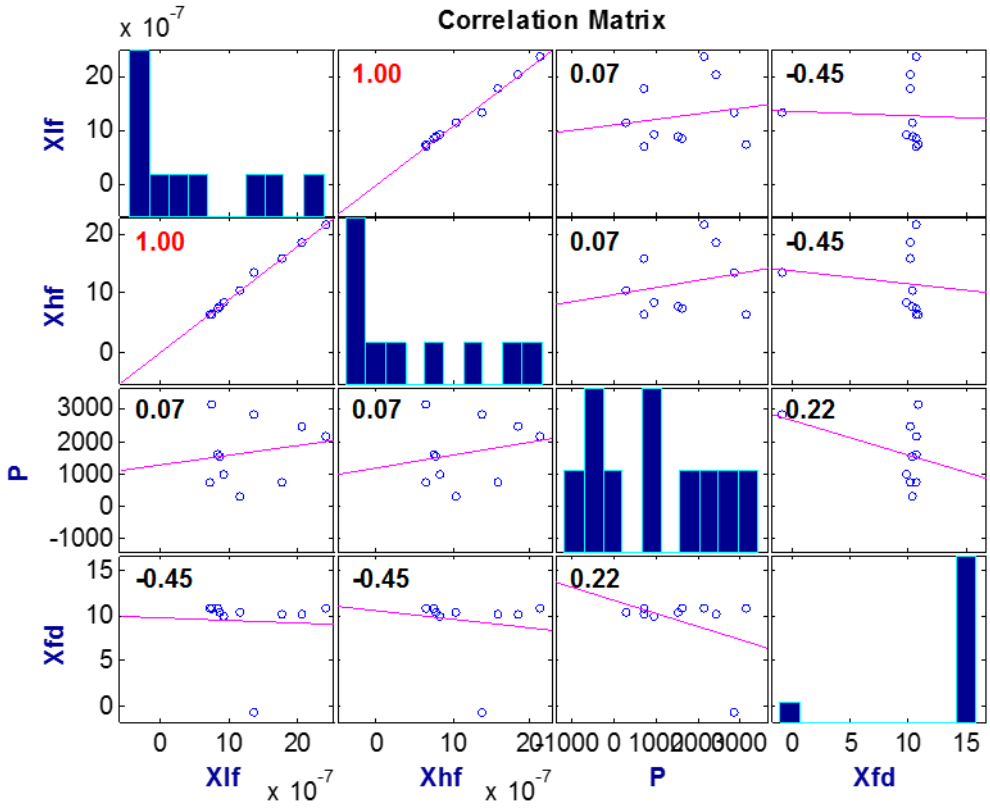

Figure 33: Results of the Spearman correlation (Line2_B, Perdika2)

Integration of Results

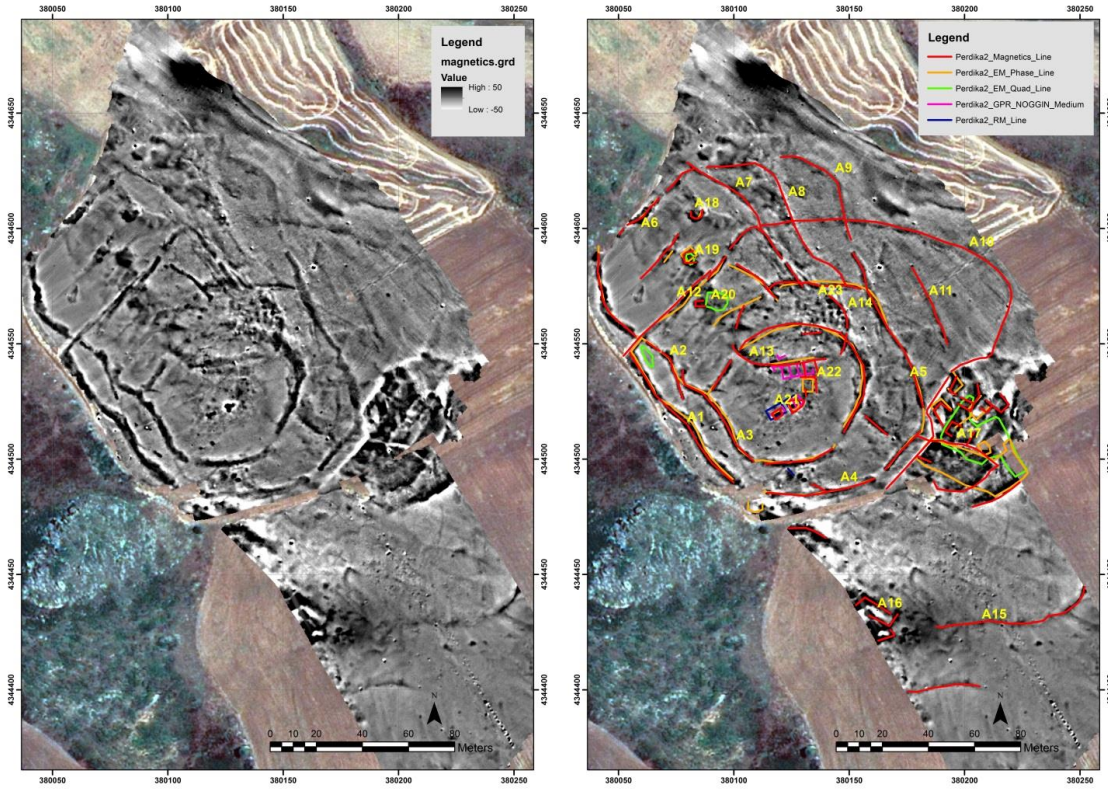

Figure 34: Compilation of anomalies on geomagnetic data

Geophysical survey at Perdika 2 revealed a complex system of enclosures different from the rest of the prehistoric sites that have been surveyed until now. Magnetics (SENSYS) and electromagnetics (GEM-2 and CMD) covered the largest area of the site, and both were illuminating in terms of the expansion of the site both on the top of the plateau of the hill, as well as along the sloping terraces of it to the east and the south.

The site consists of a number of (stone structured?) enclosures, most of which are approximately 2 m wide. The internal one, A3, seems to confine the core of the settlement (63 m x 55 m). An internal wall (A13) divides the core of the settlement into two sections. Adjacent to the southern part, there is a series of about 4-5 contiguous structures (A22) with dimensions of about (4.5 m x 3.5 m). The structures appear clearest in the GPR NogginPLUS measurements and were manifested as strong reflectors located at medium depth (~70-80 cm below the topsoil). Similar stone built structures (A21) have been identified by almost all methods at the center of the settlement. The specific structures are larger from the above and are indicated as high resistance targets. Both the magnetic data (SENSYS) and the magnetic susceptibility measurements of GEM-2 indicate the particular features as thermal (magnetic) targets, suggesting intense burning. Two gates, about 6 m wide, appear to the northwest and southeast sections of the enclosure, opposite one another, and moving along a straight line to the south another gate of similar dimensions appears to the outward enclosure (defined by A1/A4/A5/A9). This outer enclosure seems to encircle the settlement in a kind elliptical rectangle shape (151 m x ~100 m), without following the iso-elevation lines to the east, where the sloping surface of the hill appears to be more abrupt. Between the northern enclosure (A6) and the inner enclosure (A3), more enclosures appear along the plateau of the hill. The most notable one is A12, which divides the northern section of the site into two sectors with an opening at the eastern end. With the exception of the isolated targets A18,

A19 and A20, which are also associated with burning activities, the rest of the region is relatively quiet. The same holds for the rest of the area within the core of the settlement. Some dispersed strong magnetic values appear at the area of A23, but the extreme values of them show up at A17. Even though this area is somewhat fuzzy in terms of the magnetic signals, it is possible that we may have a concentration of large structural remains within a region of about 30 m x40 m. The same region exhibits high values of the soil conductivity (GEM-2). Anomaly A16 to the southwest constitutes another locus of intense values of the vertical magnetic gradient. Both of the above regions are located away of any concentrations of rocks or bedrock appearances. Finally, two more enclosures are suggested from the magnetics data to the south (A15) and to the east (A10) of the survey area.

Given the location and the plan of the site having multiple enclosures and a limited number of structural remains, it is most probable that the specific landscape was used for animal husbandry and/or agricultural activities – even if the second is less likely, since Perdika 1 is located close to a meander and flat terrain which was ideal for cultivation. Acting as a kind of a large farmstead or pastoral farming complex, the internal divisions of the settlement may have been used to confine the animals when they were released on the open landscape for grazing. Similar kinds of facilities, but of much smaller scale, have been excavated at the site of Kanalia 2 (Adrimi 2013). Perdika 2 is definitely of much larger dimensions consisting of a multi-complex system of curving enclosures that may have been constructed for the confinement of the stock or/and for diverting ground water coming from rainfalls. No one could also reject the hypothesis that the smaller internal "empty" spaces around the small structures could have functioned as small gardens to support a complementary subsistence strategy of the dwellers.

It still remains unknown the relation between the dense habitation settlements of Perdika 1 (located about 1 km to the south) and the more pastoral/agricultural oriented settlement of Perdika 2. If there was a connection between the two sites, this would definitely have been based on a common organization scheme.

Figure 35: A tentative reconstruction of anomalies draped over satellite imagery

The P lateral variations observed in Perdika 2 suggest that the core of anthropogenic activity was carried out inside the innermost enclosure (Figure 32), especially within its northeastern most area. If compared with the P results, the MS analysis did not show such a clear area of enhancement. Rather than burning activities, the very clear cluster of enhanced P may be related with accumulation of organic matter and its fixation into the soil, pinpointing towards the direction of livestock and the products of animal husbandry.

The enclosures targeted with the auger generally reached fairly flat stone at 0.35-0.5m depth (Figures 26 and 27) and resulted in relatively high χ_{lf} (~1.2E-06 m^3kg^{-1} in Point 26 and ~2.6E-06 m^3kg^{-1} in Point 11) and high FD values (9% and 10% in Points 26 and 11 respectively). Taking into consideration the MS results and the presence of red sandstone in the area, these enclosures detected with the magnetometer survey may be the foundations of wall-enclosures, built using the local flat red sandstone. The soil collected at the location of the structures detected with the GPR survey resulted in slightly higher χ_{lf} and FD values >10%. These results suggest that the structures detected may be foundations built using the same type of local rock, containing also higher quantities of mixed enhanced anthropogenic soils.

The results of Point 5 and 6 (on line 2), targeting a positive magnetic gradient anomalies, were more difficult to interpret. This feature was significantly deeper and characterized by a sequence of clay-chalk-red sand deposits. Point 5 was especially interesting because after the superficial horizon the magnetic susceptibility decreases but then increases at the depth of 50 cm, arriving to the same levels of the enclosure that was sampled in points 26 and 11.
Whilst the main anthropogenic activity seems to be happened within the innermost enclosure, the results of Point 32 (Figure 28) indicate a high percentage in SP grains and suggests some sort of human activity (e.g. possible burned soils) and the area immediately outside of the main enclosures.

Site Bibliography

Αδρύμη Β. 2013. Αγρότες Και Ψαράδες «Παρά Καλλίναον Βοιβίαν Λίμναν» ΑΝΑΣΚΑΜΜΑ, no 6 (σελ. 49 - 62)

Βουζαξάκης, Κ. 2008α. *Γεωγραφικά πρότυπα και θεωρίες του διακοινοτικού χώρου στη Νεολιθική Θεσσαλία.* Διδακτορική Διατριβή. Τμήμα Ιστορίας και Αρχαιολογίας. Α.Π.Θ. http://invenio.lib.auth.gr/ record/114226?ln=el

Βουζαξάκης Κ., 2009. *Νεολιθικές θέσεις στη Μαγνησία. Ανασκόπηση – Ανασύνθεση δεδομένων,* στο Αρχαιολογικό Έργο Θεσσαλίας και Στερεάς Ελλάδας 2 (2006), τ. Ι, σελ. 61-74.